This document was prepared in conjunction with work accomplished under Contract No. DE-DE-AC09-76SR00001with the U.S. Department of Energy.

DPST-79-402

CHARACTERIZATION OF INCINERATED SOLID WASTE ASH CONTAINING PLUTONIUM

S. M. SANDERS, Jr.

JULY, 1980

E. I. du Pont de Nemours & Co.
Savannah River Plant and Laboratory
Aiken, SC 29808

PREPARED FOR THE U. S. DEPARTMENT OF ENERGY UNDER CONTRACT DE-AC09-76SR00001

SUMMARY

The ash produced by incinerating combustible solid waste is composed of fragile aggregates of small (<2 μm diameter) particles. The size of aggregates in an aerosol resulting from this ash will depend more on the circumstances causing the aerosol than on the incineration of the waste to produce the ash. Studies reported in the literature indicate that any aerosol left undisturbed for a few minutes following its formation will consist of particles having a geometric mean diameter ranging from 0.4 to 1 μm with an average geometric standard deviation of 2 due to coagulation and sedimentation.

Plutonium will be distributed throughout the ash as small discrete concentrations. Thus, many of the smaller particles will contain undetectable quantities of plutonium. The proportion of those with plutonium to those without plutonium will depend on the overall concentration.

At concentrations of about 10 μCi/g, most particles >6 μm in diameter will contain plutonium, however, some plutonium present in particles >20 μm in diameter may not be detectable.

CONTENTS

LIST OF TABLES

LIST OF FIGURES

INTRODUCTION

When combustible solid waste is burned in an incinerator, inorganic elements end up as ash. The elemental composition and, to some extent, microscopic appearance of the ash will depend on the incinerated material. If plutonium is present, it will also become part of the ash. A knowledge of the physical properties and chemical composition of ash from the burning of solid waste containing soluble plutonium is essential to the evaluation of the hazards from such an operation.

A standard mixture of combustible materials, characteristic of solid waste, was spiked with soluble plutonium nitrate and burned by the Solid Waste Technology Group. The properties of ash particles produced by this operation were measured to support their studies of solid waste combustion.

POTENTIAL AEROSOL FORMATION

The aerosol resulting from a release of solid waste ash to the environment must involve what happens to the ash after it is released.

Ash Formation

The ash residue is composed of small particles, <2μm in diameter, sintered into large fragile aggregates by the combustion

of waste material. As the waste material is heated, volatile organics evaporate and the material begins to darken as the not-so-volatile organics begin to oxidize to carbon. At temperatures above 500°C, the carbon oxidizes to carbon dioxide. A lacy network of white inorganic ash, more or less coherent, forms as the carbonaceous material oxidizes away. This network may be recognizable as paper, cotton, or plastic ash because the basic structure remains. Near 1000°C, the sintering point is reached. The lacy network begins to collapse into white glassy particles which may include gas bubbles. The composition of the different ash materials is not the same. Thus, some of the glasses may become fluid enough to release the trapped bubbles and produce clear glassy spheres. If not agitated during this process, the elemental compositions of the particles should reflect those of the initial material.

The size of the sintered aggregates of ash particles released to the environment will depend on the circumstances of the release and the treatment of the ash before, during, and after the release. Some aggregates may remain whole; others may be pulverized into particles too small to bear any structural information.

Aerosol Properties

When dispersed into the atmosphere, some particles, having the proper size and density to produce an aerosol will remain suspended. An aerosol is, by definition, a mixture of gases and particles that exhibit some stability in a gravitational field(1).

Aerosol particles are currently classified into three modes: those with diameters <0.1 μm in the nuclei mode, those with diameters between 0.1 and 2.0 μm in the accumulation mode, and those with diameters >2.0 μm in the coarse mode (2). Particles in the nuclei mode are formed in nature by the condensation of low vapor pressure substances such as metallic vapors or partially oxygenated aromatics. Particles of the nuclei mode (e.g. Aitken nuclei) are transformed into particles of the accumulation mode by either gas-particle or particle-particle interactions. Particle-particle interactions or coagulation is governed by Brownian diffusion and occurs very rapidly. At concentrations exceeding $10^8/cm^3$, aggregates of small primary particles are formed within milliseconds. Because particle size distributions in aerosols are rarely monodispersive, coagulation usually occurs between unlike size particles.

Coarse particles arise primarily from mechanical processes, both naturally (windblown dust, sea spray, etc.) and anthropogenically (fly ash, comminutive processes, etc.). Most coarse particles are emitted close to the earth's surface, where they are removed by gravitational settling and washout before being transported very far.

Particles in the accumulation mode are not strongly affected by either coagulation or settling and are transported long distances (about 10^3 km). The distribution of aged particles tends to be unimodal, the nuclei mode particles having been removed by

coagulation and the coarse particles by settling. Measured distributions of aged particles have a geometric mean size by volume or mass ranging from 0.4 to 1 μm, with an average geometric standard deviation of 2 (3 and 4).

Thus should solid waste ash aggregates be released and broken and its particles dispersed into the environment, within minutes, the smaller particles will coagulate with each other and other particles in the atmosphere and the larger particles will settle out due to the influence of gravity. Only those in the accumulation mode, between 0.4 and 1 μm in diameter, will remain in the resulting aerosol.

COMPOSITION OF COMBUSTIBLE SOLID WASTE AND ITS ASH

The amount of plutonium in each ash particle was determined by observing fission-fragment tracks produced by it in a polycarbonate film. The probable source of selected particles was appraised by their microscopic appearance under a scanning electron microscope and elemental composition determined by X-ray energy spectrometry. To do this some information about the composition of the waste and its ash was needed.

The Waste Composite

Solid combustible waste from plutonium facilities consists of an indeterminable mixture of objects made of paper, plastics, rubbers, cotton, and adhesives. To simulate a representative sample of such waste, five components, listed in Table 1 with the weight percents of the mixture, were shredded and mixed.

The Ash

Elemental analyses of the ash from each of the separate components were made by spark source mass spectrometry (5). Ten-gram batches of waste from each component, except the polyethylene bags, were weighed into a 250-mL porcelain crucible. The samples were pyrolyzed in air using a Meeker burner. The crucibles were placed in a preheated muffle furnace and maintained at 1000°C for one hour. To provide sufficient ash from polyethylene bags, a 100-g batch was weighed into a porcelain dish. After pyrolysis, the residue from the polyethylene bags was transferred to a crucible before being placed in a muffle furnace. This procedure produces ashes which are light, very fragile aggregates of very small particles (<2 μm in diameter). The size of these aggregates depends on how the ash is handled.

The ash from the cellulose, latex, and polyethylene components represented less than 1.5% of the total weight of the uncombusted material. The ash from the polyvinyl chloride shoe covers and neoprene gloves represented between 8 and 10% of the weight of the initial material and thus would be expected to contribute most of the ash material.

Elemental analysis of the ash from each of the separate components was made by spark source mass spectrometry. The results of these analyses are given in Table 2. Calcium concentrations were found in the ash from only three components: in the cellulose component from calcium hypochlorite used to

bleach the cotton, in the polyvinyl chloride component from calcium sterate used as a stabilizer, and in the latex component from calcium used as a reinforcing agent. Titanium concentrations were found in the ash from only two of the three components containing calcium: In the cellulose component from titaium dioxide used as a filler in the paper in atomic wipes, and in the polyvinyl chloride component from the white colorant and ultraviolet stabilizer in the shoe covers. Iron concentrations were found in the ash from only the cellulose and polyethylene components. Zinc concentrations were found in only the ash from the latex and neoprene components. In the ash from the polyethylene bags, high concentrations of silicon were found from the silica gel catalyst substrate used to manufacture polyethylene. Ash from the neoprene component contained high concentrations of magnesium due to MgO used as an accelerator to increase the rate of vulcanization. From this information a key, given in Figure 1, was developed to identify the source of individual isolated particles of ash.

Test Analyses of the Ash

To see if the source of ash particles could be identified by x-ray energy spectrometry, ash aggregates were taken from each of the different components. These aggregates were crushed on pyrolytic graphite planchets. The resulting particles were then photographed using the scanning electron microscope and their elemental composition determined by x-ray energy spectrometry.

The elemental composition of particles of ash from the cellulose component varied considerably from one particle to the next as well as from the composition found by spark source mass spectrometry. Figure 2 shows three magnifications of cellulose component ash and the five particles selected for analysis. Figure 3 is a picture of a 5 μm diameter particle (particle a in Figure 2). Below the picture is an X-ray energy spectrum showing a high concentration of silicon. From this and its iron peak, this particle might be considered to be ash from polyethylene if it did not have calcium present. Yet, there should be titanium present to classify it as ash from the cellulose component. The top particle in Figure 4 is almost entirely iron. Particles below it have high silicon concentration and less iron. Calcium is not observed except in the bottom particle. Atomic wipes contain a layer of polyethylene and this group of particles may have come from this layer rather than the cellulose of the cotton and paper present.

The elements found in polyvinyl chloride ash were more uniformly distributed and correspond to those found by spark source mass spectrometry. Figure 5 shows two magnifications of ash from polyvinyl chloride shoe covers and the X-ray energy spectrum from one particle showing that it was composed principally of calcium and titanium and that no iron was present. Figure 6 shows two higher magnifications of the same ash. The spectrum of a particle near the outer boundary of particles

indicates that it also contains calcium and titanium and no iron. The spectra above the pictures are those of the background among the particles and beyond the boundary.

The key developed from spark source mass spectrometry can also be used to identify ash from latex gloves. The top two pictures in Figure 7 are different magnifications of ash from latex gloves. The bottom pictures are still higher magnifications of areas marked by the two small squares in the upper right picture. The larger square is the area covered in Figure 8. With the exception of a small amount of iron in one particle near the boundary in Figure 8, all agree with the elemental compositions found by spark source mass spectrometry.

Figure 9 shows three magnifications of ash from polyethylene bags. The elemental composition of the ash from polyethylene, like that from cellulose, is not uniform and does not match what was found from spark source mass spectrometry. The bottom square in Figure 9 is covered in Figure 10. Although three of the four particles analyzed in this figure show major silicon peaks, three also contain titanium, two contain a trace of zinc, and one contains calcium, which makes its elemental composition resemble that of cellulose ash. Figure 11 covers the area of the small square in Figure 9. In this figure, one particle contains a high titanium concentration. The other is a siliceous diatom frustule. Diatoms are a cheap and inert filler for plastics. Although milled for this use to fine fragments, the characteristic shape is still apparent.

Ash particles from the combustion of neoprene, like those from polyvinyl chloride and latex, are uniform as to their elemental composition and can be identified by their relatively high magnesium concentration. Figures 12 and 13 show ash from incinerated neoprene gloves at various magnifications. All analyses but one show high magnesium and silicon concentrations. One particle contained sufficient aluminum to mask the magnesium.

Thus, measurements using ash from individual components indicate that the ash from polyvinyl chloride shoe covers, latex gloves, and neoprene gloves can be identified from their x-ray energy spectra. Ash from atomic wipes and polyethylene bags cannot be distinguished with certainty by their elemental analyses.

PLUTONIUM DISTRIBUTION IN ASH

To see how plutonoum is distributed in ash from incinerated solid waste, plutonium was added to a sample of the standard mixture. The sample was incinerated, the ash crushed, and ash particles with and without fission-fragment tracks were separated. The source of each particle was then identified by x-ray energy spectrometry.

Sample Preparation

Two microcuries of $^{239}Pu(NO_3)_4$ in 1M HNO_3 was added to 5 g of the standard mixture, described in Table 1, to simulate combustible solid waste. This sample was pyrolyzed in air and ignited for one hour at 1000°C as the individual components had

been done earlier. A 1-mm diameter aggregate of this ash was placed in a 1-mL Thomas tissue grinder with a Teflon pestle. The aggregate was ground in 1 mL of 40% (v/v) 1,2-dichloroethane in dichloromethane solution. Polycarbonate was added to the solution and the solution was evaporated on a 50-mm square glass plate to form a clear polycarbonate film containing the particles. The cast film was irradiated with a measured thermal neutron fluence in the order of 9×10^{14} neutrons/cm^2. Fission fragments produced tracks when the film was etched for 10 minutes in 6N NaOH at 52°-55°C (6-9) which radiated from imbedded particles containing plutonium.

Particle Selection and Mounting

About 60% of the particles produced fission fragment tracks in the polycarbonate film, indicating that they contained ^{239}Pu. The other 40% produced no tracks.

Eleven particles producing fission-fragment tracks and twelve particles having no tracks were photographed using a light microscope, excised from the film, and mounted on a pyrolytic graphite planchet. Excess polycarbonate film was dissolved and removed from around the particles using 1,2-dichloroethane. Each particle was then photographed using a scanning electron microscopy

Particle Identification

The elemental composition of each particle was determined by x-ray energy spectrometry and this information used to identify the component of the standard mixture which produced it.

The X-ray energy spectra for these particles are given in Figures 14 and 15 along with photographs taken of the particles with light and scanning electron microscopes. To aid in comparing the results, the background was subtracted from the height of each peak and the sum of the resulting heights was normalized to 100. From the relative abundance of the elements present in each ash particle, the most likely component producing the ash was selected using the key given in Figure 1. The elemental composition of each particle of ash and the component of the waste from which it appears to have originated are given in Tables 3 and 4.

Plutonium Content

The apparent plutonium content of each particle was measured by counting the number of fission-fragment tracks surrounding it. From past experience (8), one fCi (10^{15} Ci) of low-irradiation plutonium containing 94% ^{239}Pu should produce about 26.5 fission fragment tracks when exposed to a fluence of 9×10^{14} thermal neutrons per cm^2. Thus, the number of fCi in each particle was determined by dividing the number of fission fragment tracks by 26.5.

Particle Size and Weight

The conventional method of using particle diameter to determine volume and mass could not be used with these ash aggregates, for what initially was selected as a single, almost spherical particle broke apart during processing to produce many

smaller irregular shaped particles having a smaller total volume than the original aggregate. This can be seen in Figures 14 and 15 where closely packed aggregates pictured in the polycarbonate film appear as disordered clusters after the polycarbonate has been removed.

The volume of the initial particle was therefore approximated by the total volume of ellipsoids having similar dimensions as its n pieces, or

$$V = \frac{\pi}{6} \sum_{i=1}^{n} A_i B_i C_i$$

where A_i, B_i, and C_i are the lengths of the axes of the ith piece in μm. Most of the pieces were considered to be prolate spheroids (A >B=C), although some were oblate spheroids (A=B <C) and spheres (A=B=C).

The mass of the particles was calculated assuming the density of incinerator ash to be 2.4 g/cm^3 = 2.4 $pg/\mu m^3$ (10).

The specific activity in Ci/g was then calculated by taking the ratio of the activity to the mass or

$$\text{SpA. } (\mu Ci/g) = \frac{fCi}{pg} \cdot 10^3$$

For comparison, an effective radius, r, for each particle was calculated from the total volume assuming the particle to be a sphere or

$$r = \left(\frac{3V}{4\pi}\right)^{1/3}$$

In Table 5, the particles are arranged according to increasing effective radii and the calculated mass, plutonium activity, and specific activity for each given.

DISCUSSION

Before the data were critically analyzed, the plutonium appeared to be unevenly distributed with about 40% of the particles containing none. From the component source of each particle, as determined from elemental analysis, the soluble plutonium appeared to be absorbed on porous materials like cellulose (Table 3) and to be repelled from nonporous materials like polyethylene (Table 4). Thus, the plutonium was uniformly distributed at the particle level but nonuniformly distributed as the sample level.

However, the arrangement of the data in Table 5 may provide a more plausible explanation. In this table, the specific activity of plutonium appears to decrease with an increasing effective radius. This could result from the plutonium being nonuniformly distributed at the particle level.

Katcoff et al.(11) give the range of fission fragments from ^{239}Pu in air at 15°C and 760 mm Hg of between 1.8 and 2.7 cm depending on the mass number of the fragment with 2.5 cm for the most probable light mass and 1.9 cm for the most probable heavy mass. The ranges for fission fragments in polycarbonate, quartz, and PuO_2 calculated using the Bragg-Kleeman Rule are given in Table 6. Here the maximum range of a fission fragment in quartz

is 13.7 μm. Thus, a polyethylene ash particle having a radius greater than 13.7 μm would not be expected to produce fission fragment tracks from plutonium located in its center. In Table 5 none of the 12 particles selected as not having tracks have effective radii less than 7.0 μm and 9 of 12 have radii greater than 11 μm.

The specific activity of the smaller particles also appear to be what would be expected if the plutonium were uniformly distributed. Assuming that 10% of the weight of polyvinyl chloride and neoprene and 1.5% of cellulose, polyethylene, and latex is ash, the overall ash concentration of simulated combustible waste would be 4.4% if the components are proportioned according to the distribution given in Table 1. Thus, 5 g of the standard mixture will yield 0.22 g of ash. Two μCi of plutonium added to this sample would result in a specific activity of 9.1 μCi/g of ash. The specific activities given in Table 5 approach this value for only the smaller particles. As the effective radii increase the specific activity decreases. The one exception to this relationship occurred with particle number P-10 in Figure 14d. This particle was situated so that the plutonium protruded above the polycarbonate film and produced fission- fragment tracks over 100 μm from the particle.

This phenomenon can be explained geometrically by considering the plutonium to be a point source radiating fission-fragment tracks in all directions in an essentially infinite polycarbonate

medium. If the tracks form a sphere with plutonium at the center, the particle containing the plutonium will obscure some of the tracks. The fraction of the total number of tracks which will be counted, f, can be approximated by the ratio of the area of the zone of the sphere which can be seen to the total area of the sphere or

$$f = \frac{2\pi Rh}{4\pi R^2} = \frac{h}{2R}$$

where h = the altitude of the zone, and

R = the range of the tracks.

The altitude of the zone can be related to the range of the tracks and the radius of the particle, r, by

$$h = 2(R^2-r^2)^{1/2}.$$

Thus, as the radius of the particle approaches the range of the tracks, the fraction of the tracks observed approaches zero.

If the medium is not infinite and the point source of plutonium is a distance, d, above the polycarbonate surface, the altitude of the zone is

$$h = (R^2-r^2)^{1/2} - d.$$

If the medium is air above the polycarbonate rather than the polycarbonate itself, then $R>>r$ and $R>>d$. Under these conditions, $h \cong R$ and $f = 1/2$. Thus, the specific activity for this particle was calculated assuming that only half the fission-fragment tracts were counted.

To see how well these geometrical limitations to track observations fit the data, the range of the tracks were calculated from the ratio of the observed specific activity to 11.7 Ci/g, the specific activity calculated for particle number P-10, using the effective particle radius. These calculated values, which range from 4.5 to 9.6 μm are given in Table 5.

The specific activity for those particles with tracks being about the same as the specific activity calculated for the ash as a whole, supports the concept that the plutonium is distributed throughout the ash. The large particles, selected because they did not produce tracks, probably contained plutonium in locations where tracks could not be observed. There were large particles which produced tracks, which were not selected for analysis.

The plutonium was not distributed homogeneously in the ash, but as very small discrete concentrations. This concept is supported by the geometry of the track configurations and the fact that most small (<1 μm diameter) particles contained no plutonium.

TABLE I

COMPOSITION OF SIMULATED COMBUSTIBLE WASTE

PRINCIPAL INGREDIENT	ITEM	WEIGHT %
CELLULOSE	ATOMIC WIPES	28
POLYVINYL CHLORIDE	WHITE SHOE COVERS	24
POLYETHYLENE	BAGS	19
LATEX	RUBBER GLOVES	19
NEOPRENE	GLOVES	10

TABLE 2

COMPOSITION* OF ASH FROM INDIVIDUAL WASTE COMPONENTS BY SPARK-SOURCE MASS SPECTROMETRY

ELEMENT	CELLULOSE ATOMIC WIPES	POLYVINYL CHLORIDE SHOE COVERS	LATEX RUBBER GLOVES	POLY-ETHYLENE BAGS	NEOPRENE GLOVES
Mg	43	4	41	7	76
Al	3	8	-	3	13
Si	6	6	32	79	9
P	-	5	-	-	-
Ca	24	39	17	-	-
Ti	8	35	-	-	-
Fe	12	-	-	8	-
Zn	-	-	6	-	2
Ba	-	2	-	-	-
TOTAL	96	99	96	97	100

*WEIGHT PERCENT OF ALL ELEMENTS CONSTITUTING 1 WT % OF THE ASH EXCLUDING CARBON, OXYGEN, AND NITROGEN.

TABLE 3. ELEMENTAL COMPOSITION OF PARTICLES WITH FISSION FRAGMENT TRACKS

Particle	Mg	Al	Si	Ca	Ti	Fe	Cl	Component
P-1	-	9	10	44	35	3	-	Cellulose
P-2	15	18	19	19	15	2	11	Cellulose
P-3	19	-	19	18	22	2	19	Cellulose
P-4	-	7	-	41	52	-	-	Polyvinyl Chloride
P-5	-	-	5	45	50	-	-	Polyvinyl Chloride
P-6	9	7	10	29	45	-	-	Polyvinyl Chloride
P-7	11	18	21	20	29	-	2	Polyvinyl Chloride
P-8	12	14	16	27	27	-	4	Polyvinyl Chloride
P-9	16	28	42	9	5	-	-	Polyvinyl Chloride
P-10	17	20	16	18	22	-	7	Polyvinyl Chloride
P-11	-	-	87	7	-	6	-	Latex

TABLE 4. ELEMENTAL COMPOSITION OF PARTICLES WITHOUT FISSION FRAGMENT TRACKS

Particle	Mg	Al	Si	Ca	Ti	Fe	Cl	Component
S-1	28	-	72	-	-	-	-	Polyethylene
S-2	25	-	75	-	-	-	-	Polyethylene
S-3	30	-	70	-	-	-	-	Polyethylene
S-4	-	-	-	45	55	-	-	Polyvinyl Chloride
S-5	-	-	12	49	39	-	-	Polyvinyl Chloride
S-6	-	-	-	41	59	-	-	Polyvinyl Chloride
S-7	-	-	1	47	52	-	-	Polyvinyl Chloride
S-8	-	-	-	54	46	-	-	Polyvinyl Chloride
S-9	12	21	33	20	6	-	7	Polyvinyl Chloride
S-10	28	-	69	-	-	-	3	Polyethylene
S-11	-	-	-	-	-	-	100	Uncertain
S-12	-	-	-	9	-	-	91	Uncertain

TABLE 5

The Weight and Plutonium Content of Twenty-three Particles of Combustible Waste Ash

Particle Number	*Effective Radius* (μm)	*Component*	*Weight* (ng)	*Activity* (fCi)	*Specific Activity* (μCi/g)	*Track Range* (μm)
P-5	3.1	PVC	0.3	3.4	11.0	9.1
P-1	3.2	Cellulose	0.3	2.8	8.5	4.7
P-11	4.2	Latex	0.7	3.0	4.2	4.5
P-6	4.5	PVC	0.9	2.7	3.2	4.7
P-4	4.6	PVC	1.0	2.4	2.4	4.7
P-7	5.5	PVC	1.7	6.6	3.8	5.8
P-2	6.3	Cellulose	2.5	4.5	1.8	6.4
P-10	6.6	PVC	2.9	34.4	11.7*	
P-3	6.8	Cellulose	3.2	5.7	1.8	6.9
S-11	7.0	Uncertain	3.5			
S-7	7.0	PVC	3.5			
P-8	8.5	PVC	6.2	7.2	1.2	8.5
S-12	9.4	Uncertain	8.5			
P-9	9.6	PVC	8.8	7.5	0.9	9.6
S-8	11.9	PVC	14.7			
S-1	12.1	Polyethylene	17.9			
S-2	12.9	Polyethylene	21.4			
S-3	14.0	Polyethylene	27.4			
S-10	14.0	Polyethylene	27.6			
S-6	17.5	PVC	55.2			
S-5	21.4	PVC	98.0			
S-4	22.4	PVC	112.4			
S-9	26.0	PVC	176.9			

*Calculated assuming that half the fission-fragment tracks are counted.

TABLE 6

The Range of Fission Fragments in Air, Polycarbonate, Quartz, and PuO_2

Media	*Heavy Mass*	*Light Mass*
Air (mm)	19.4	24.8
Polycarbonate (μm)	12.9	16.5
Quartz (μm)	10.7	13.7
PuO_2 (μm)	4.3	5.5

FIGURE 1. KEY FOR THE IDENTIFICATION OF A COMBUSTIBLE WASTE COMPONENT FROM THE ELEMENTAL COMPOSITION OF ITS ASH.

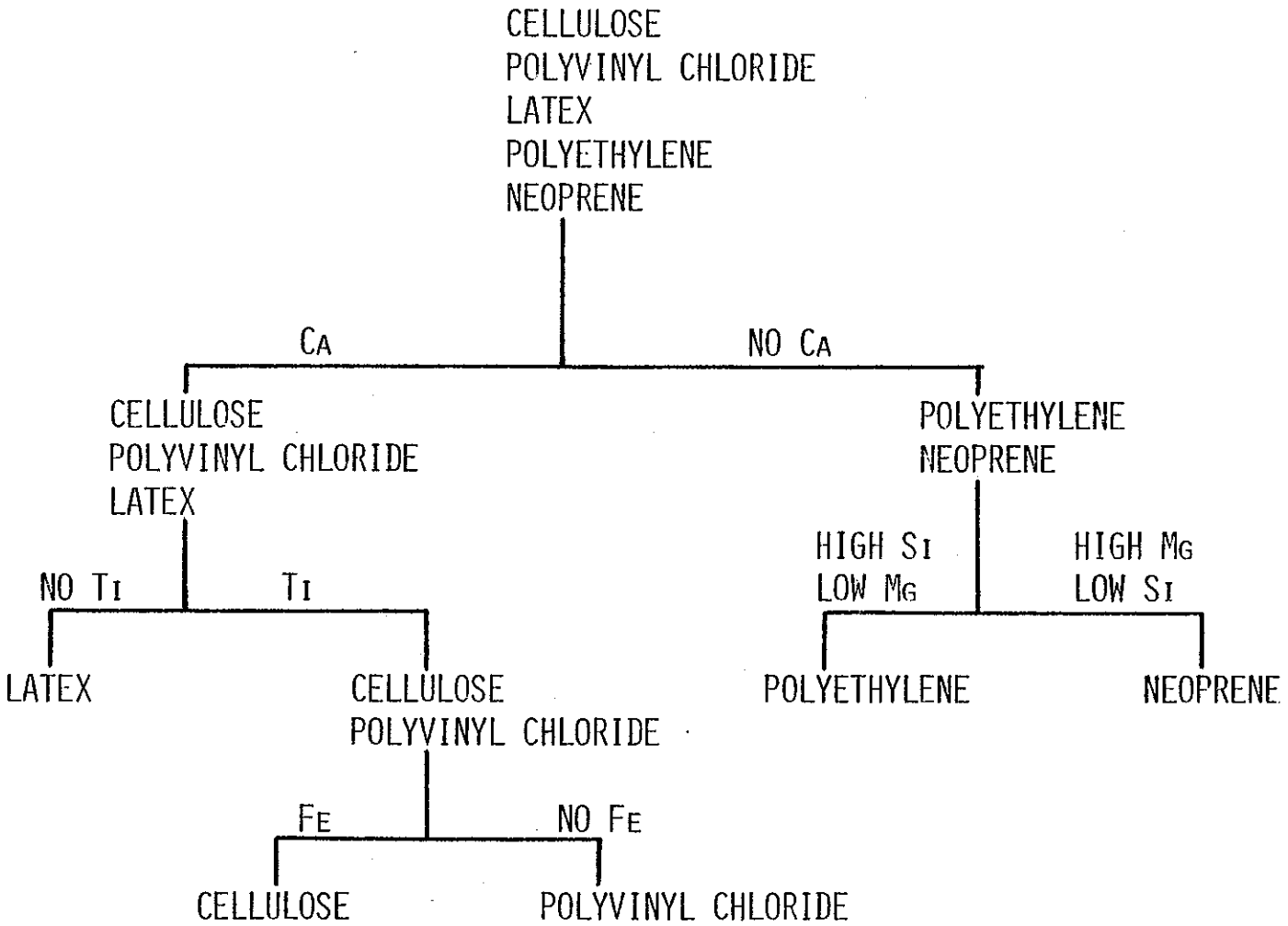

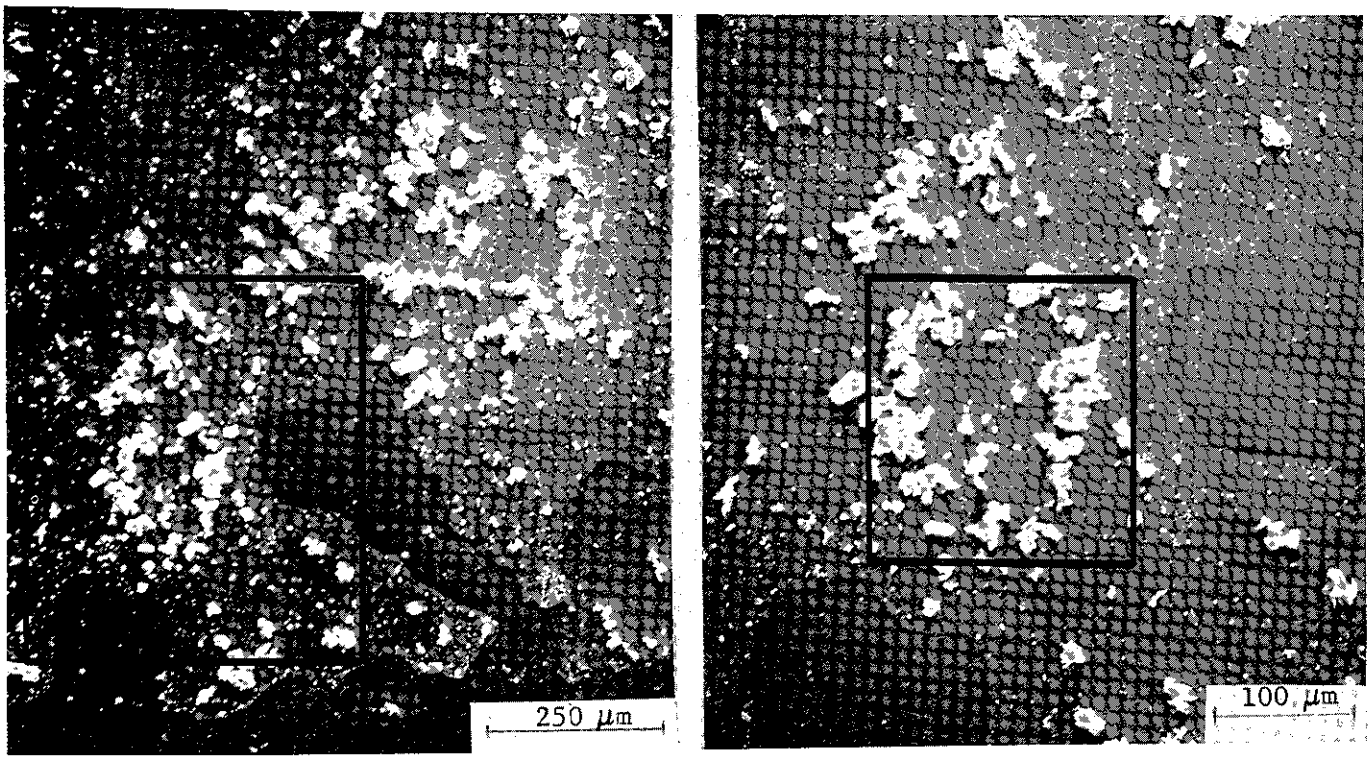

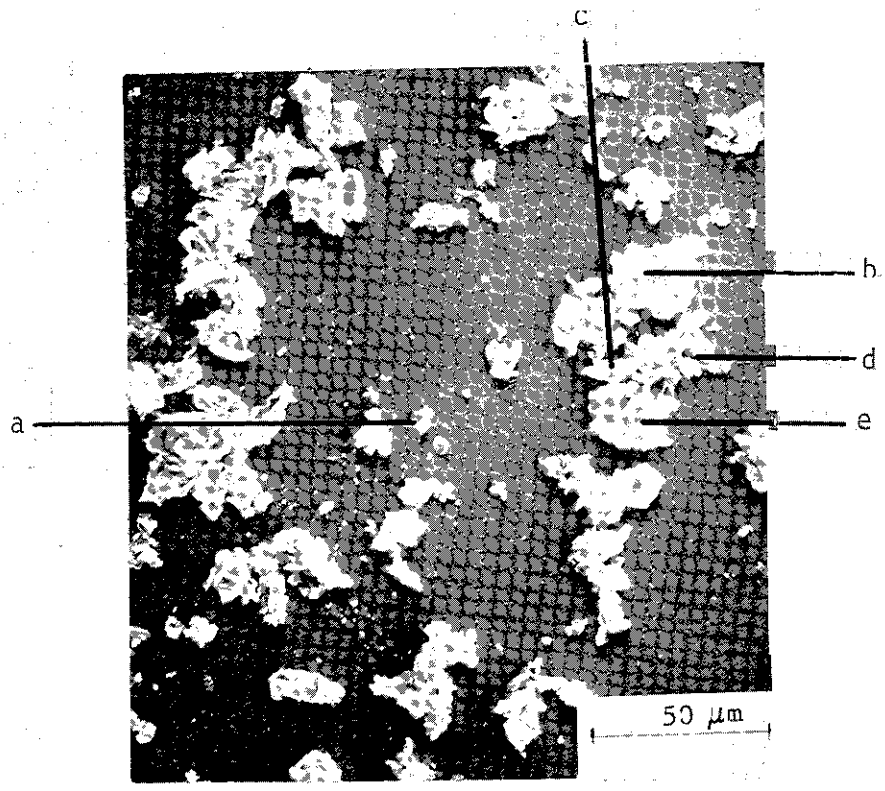

Figure 2. Incinerator ash from cellulose atomic wipes magnified 100X, 200X, and 500X showing location of XES analyses.

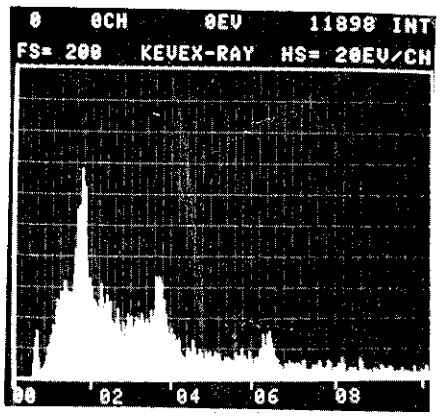

Mg, Si, Ca, Fe

Figure 3. Fragment a of incinerator ash from cellulose atomic wipes magnified 5000X.

Figure 4. Fragments b, c, d, of incinerator ash from cellulose atomic wipes magnified 5000X.

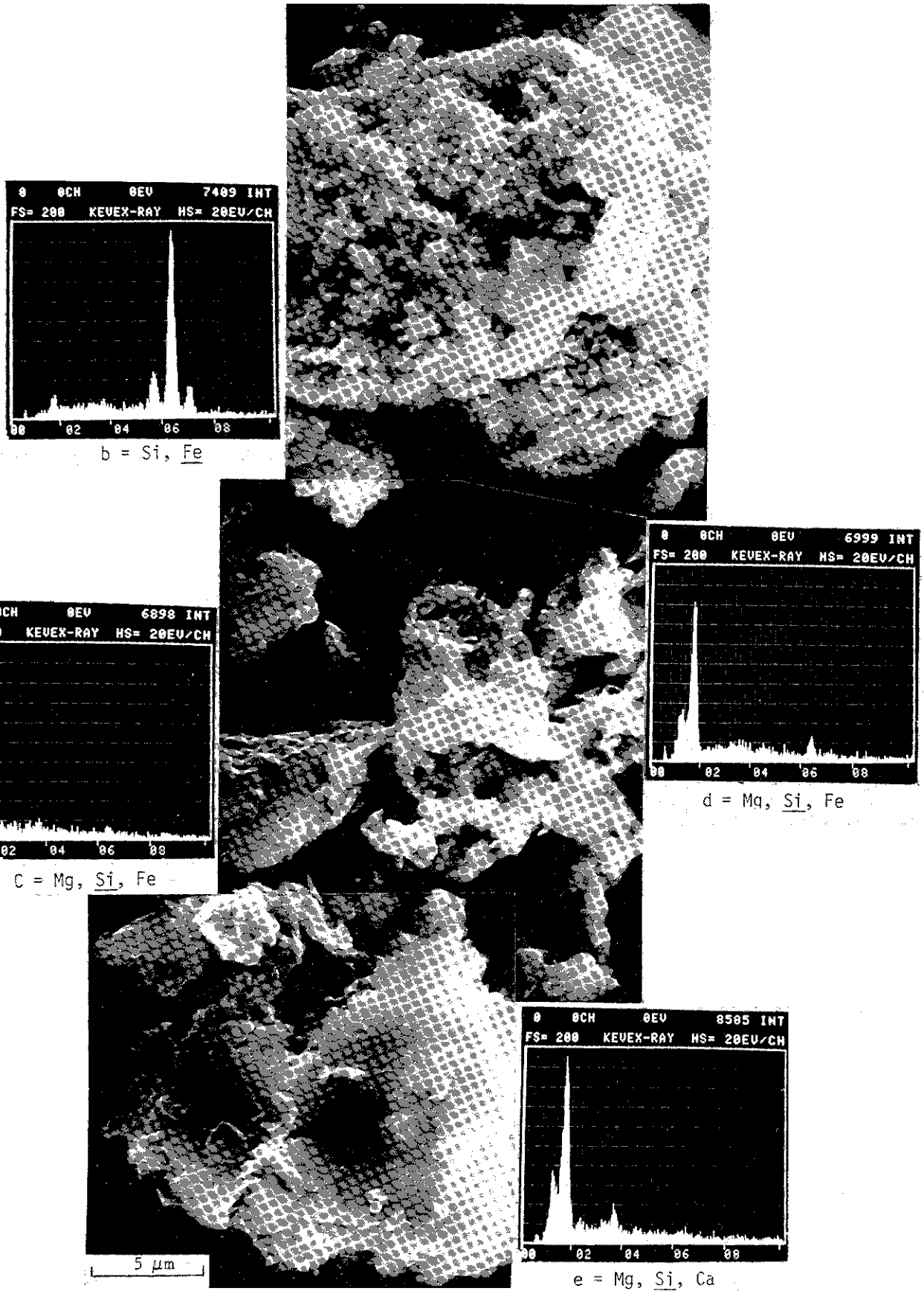

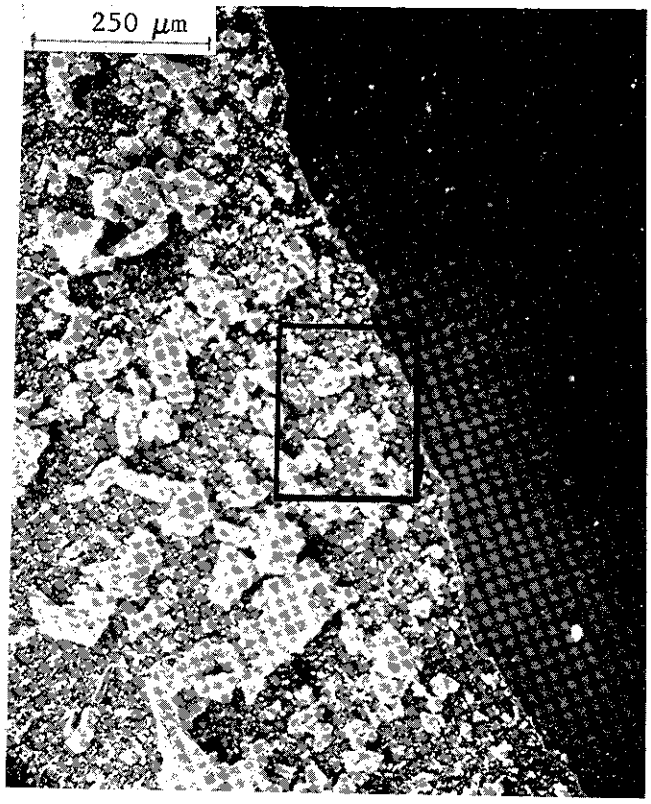

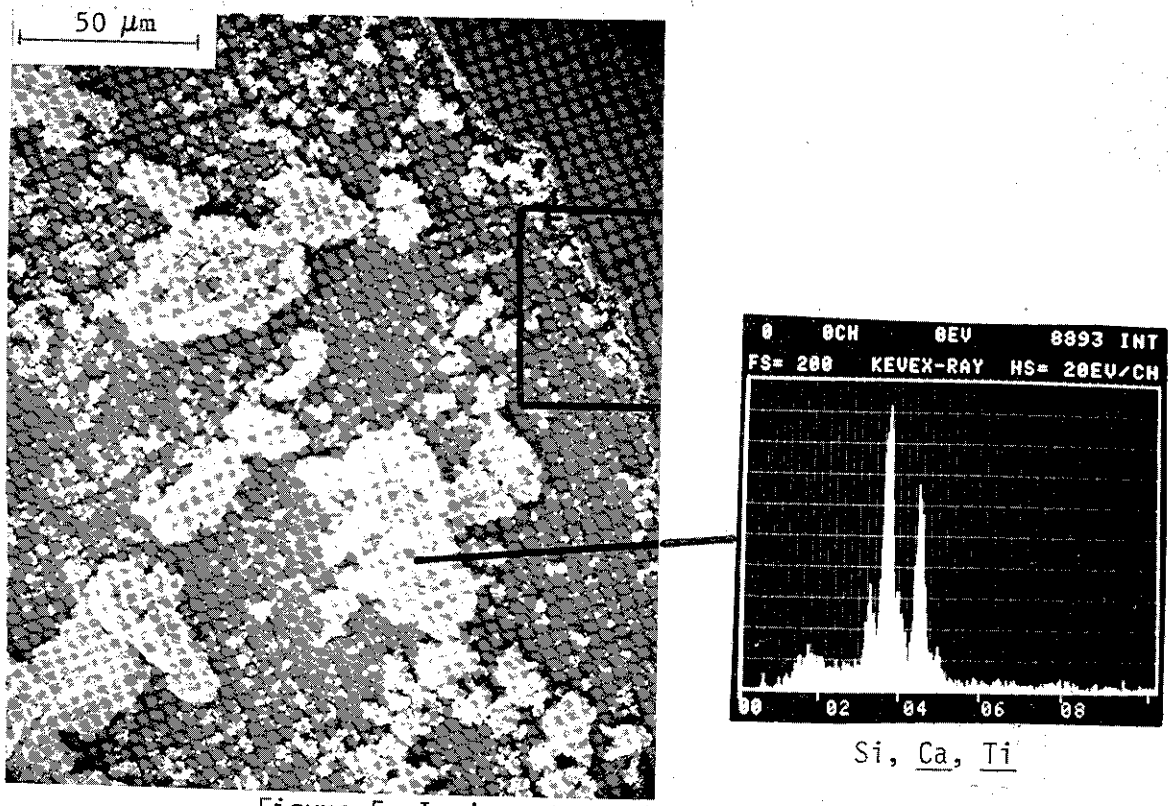

Si, Ca, Ti

Figure 5. Incinerator ash from polyvinyl chloride shoe covers magnified 100X and 500X.

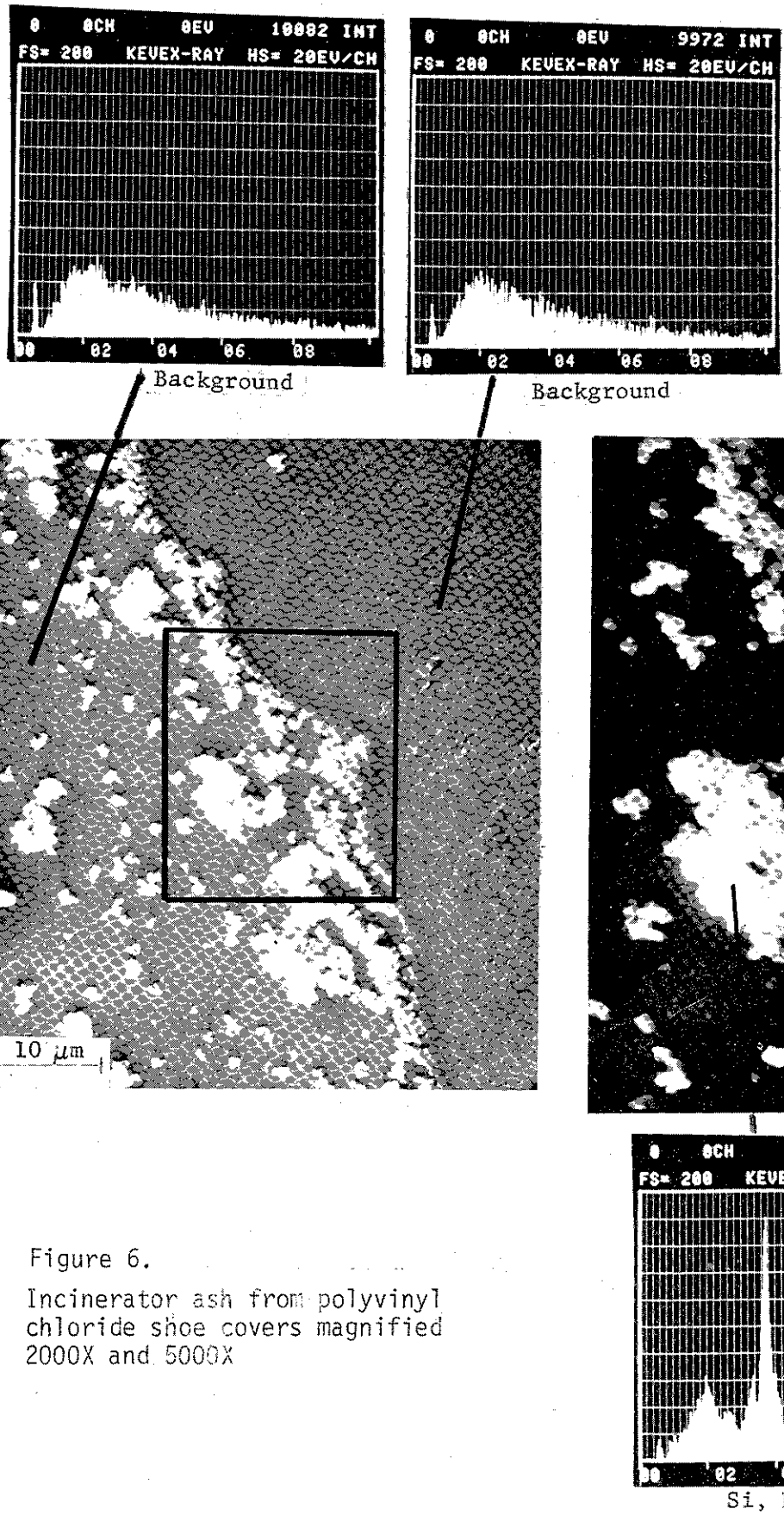

Figure 6.

Incinerator ash from polyvinyl chloride shoe covers magnified 2000X and 5000X

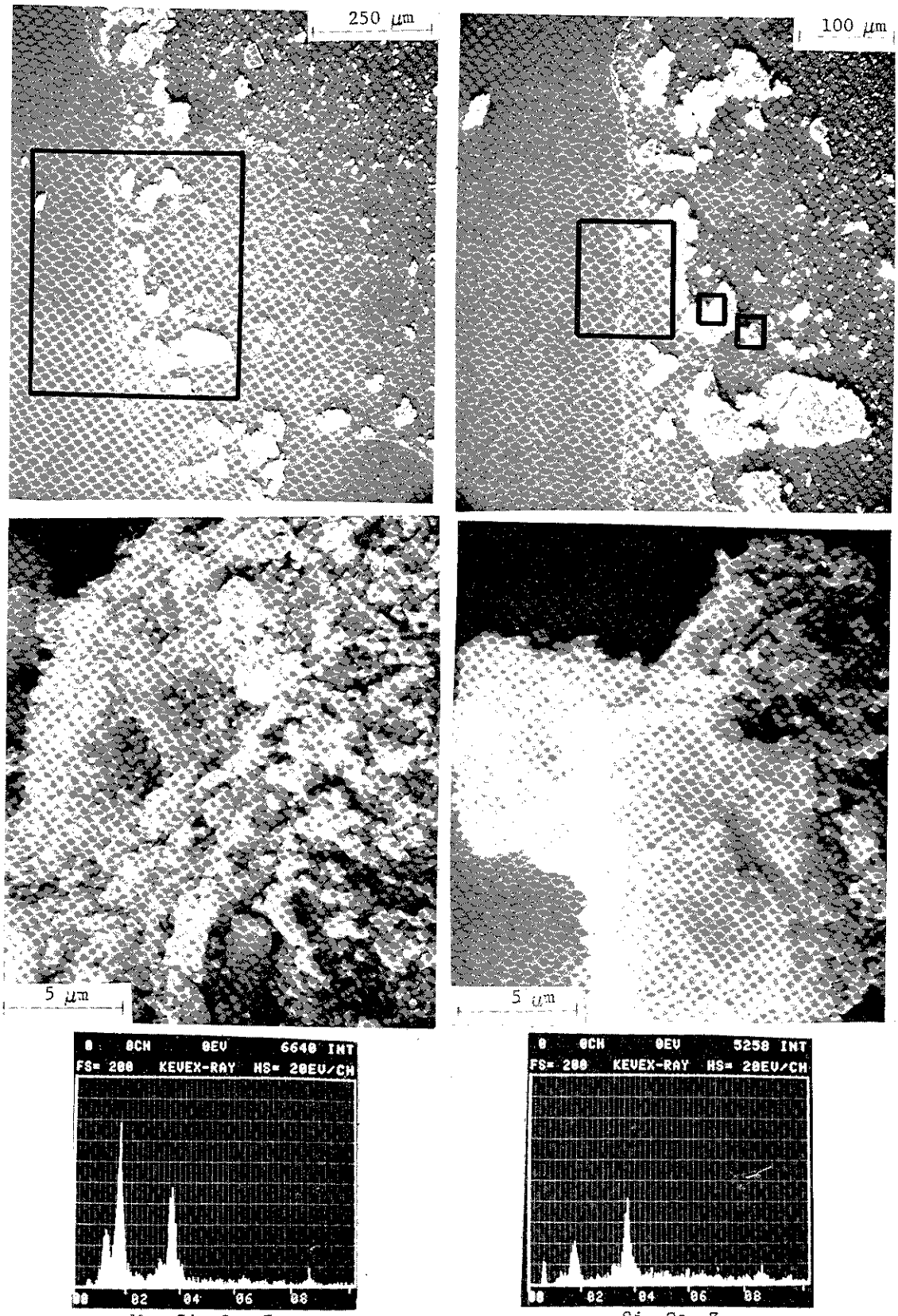

Mg, Si, Ca, Zn

Si, Ca, Zn

Figure 7. Incinerator ash from latex gloves magnified 100X, 200X, and 5000X.

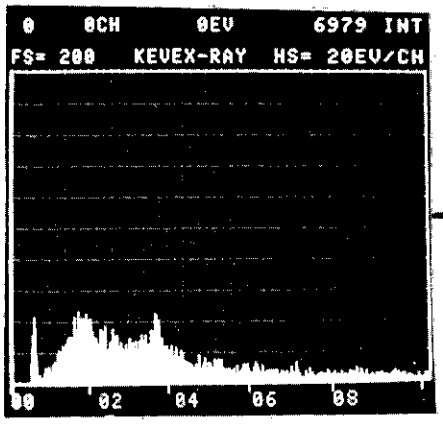

Si, Ca

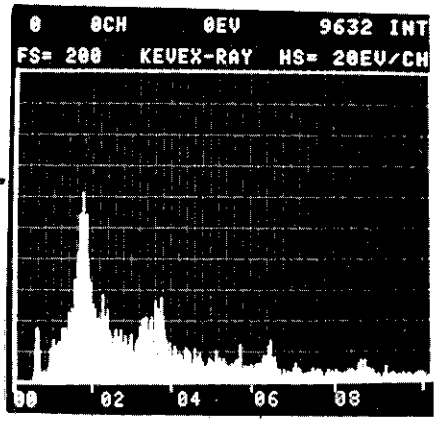

Si, Ca, Fe, Zn

Figure 8. Incinerator ash from latex gloves magnified 1000X and 5000X.

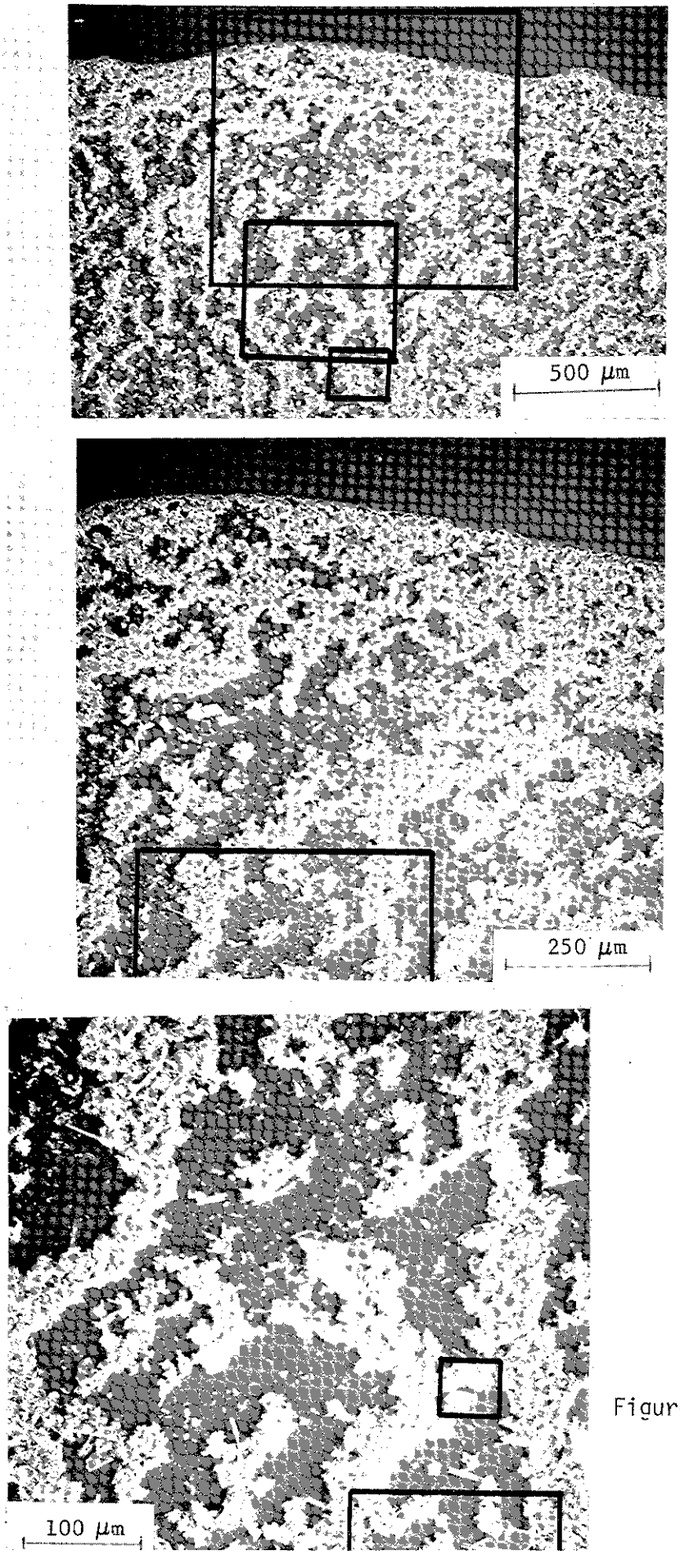

Figure 9. Incinerator ash from polyethylene bags magnified 50X, 100X, and 200X.

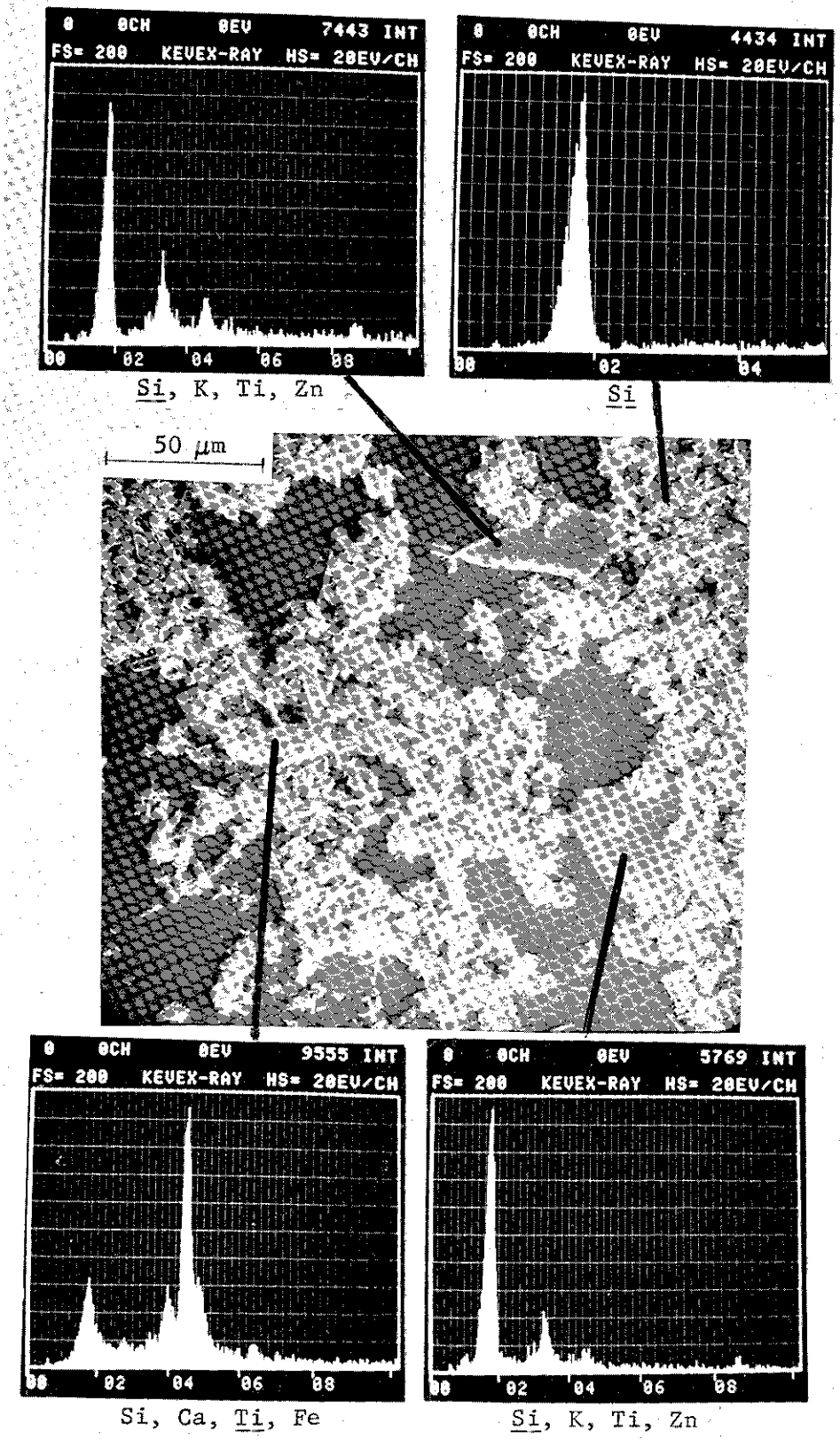

Figure 10. Incinerator ash from polyethylene bags magnified 500X.

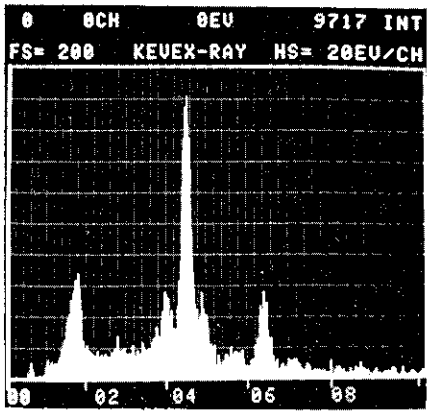

Si, Ti, Fe

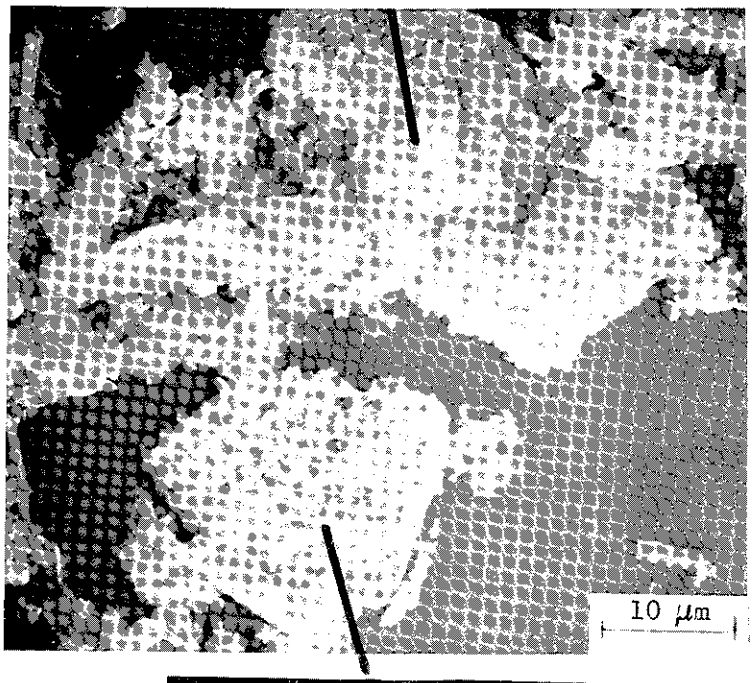

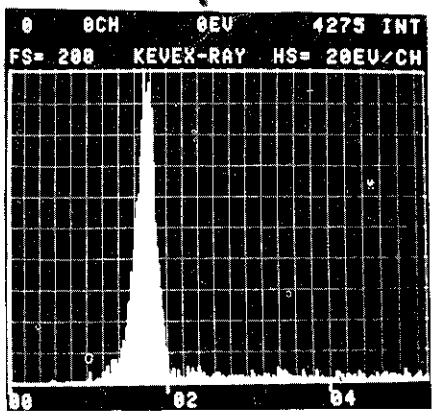

Si

Figure 11. Incinerator ash from polyethylene bags magnified 2000X.

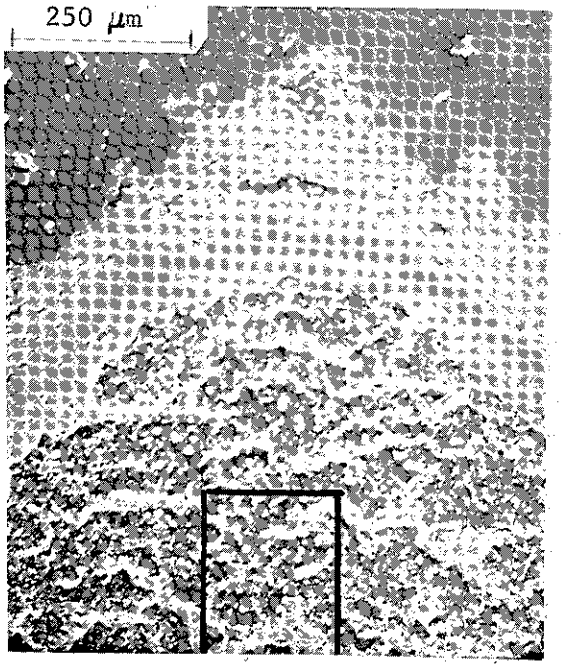

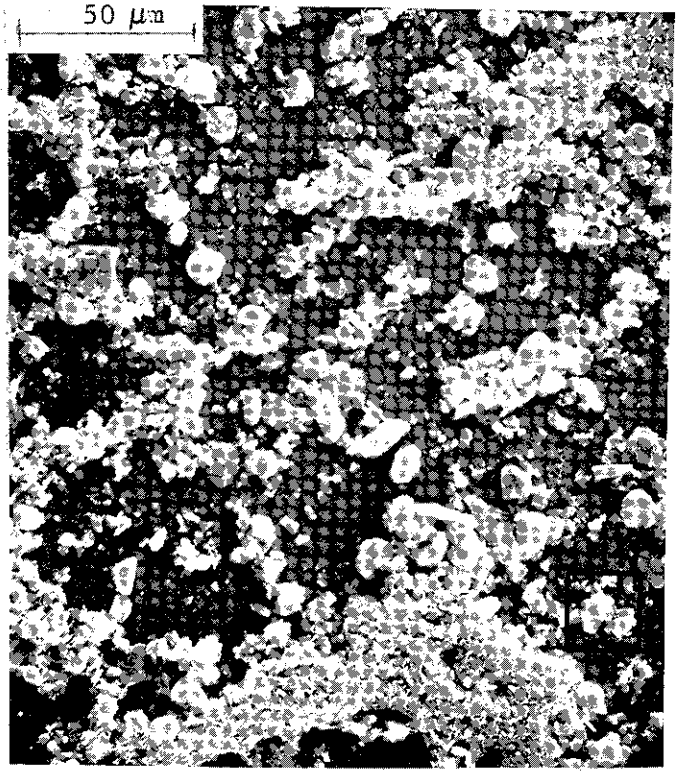

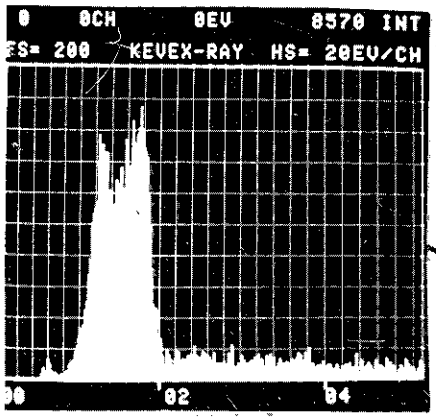

Mg, Si

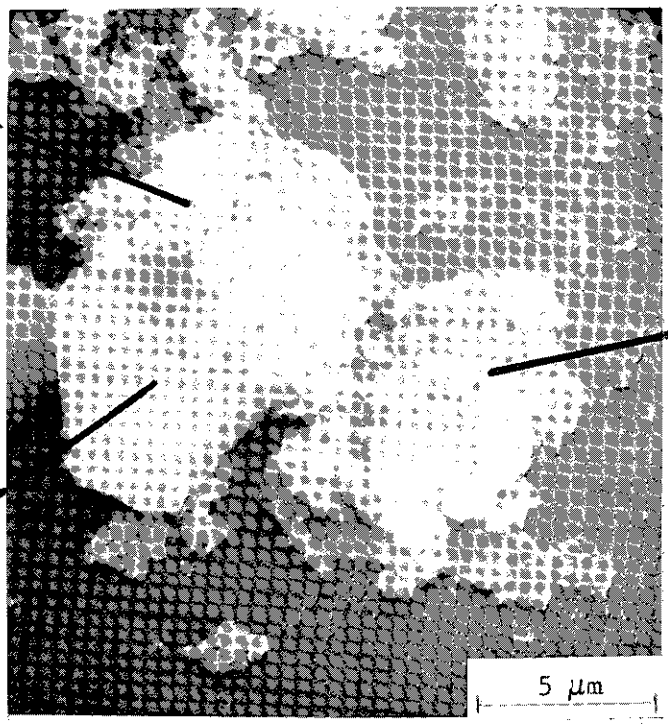

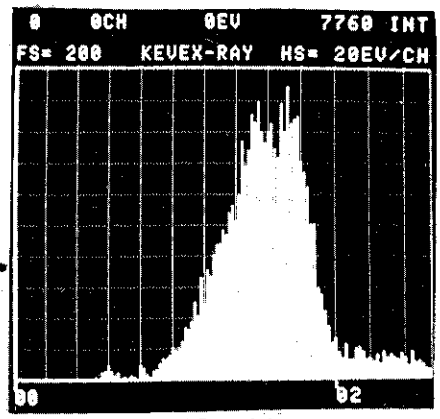

Al, Si

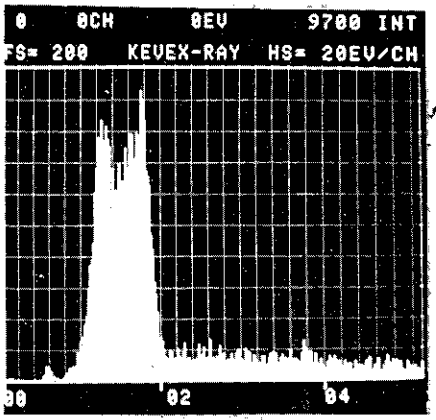

Mg, Si

Figure 12.
Incinerator ash from neoprene gloves magnified 100X, 500X and 5000X.

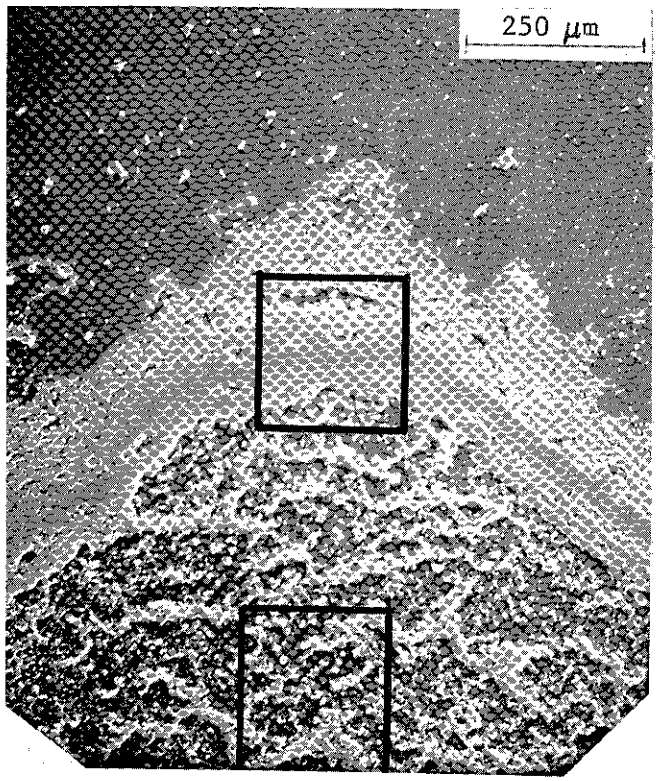

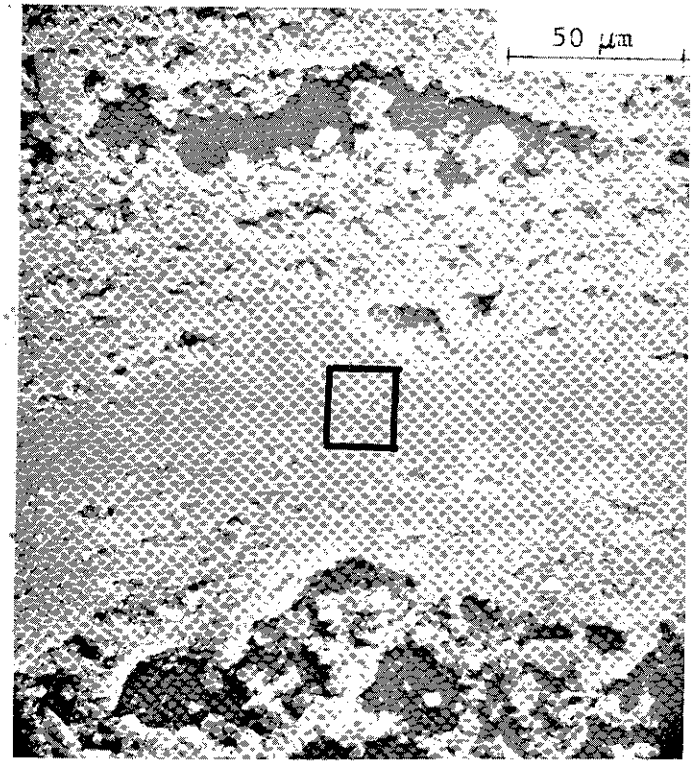

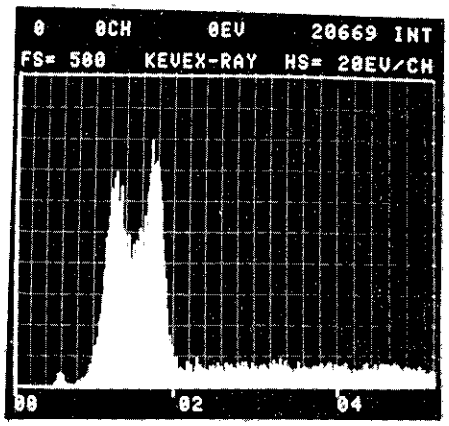

Mg, Si

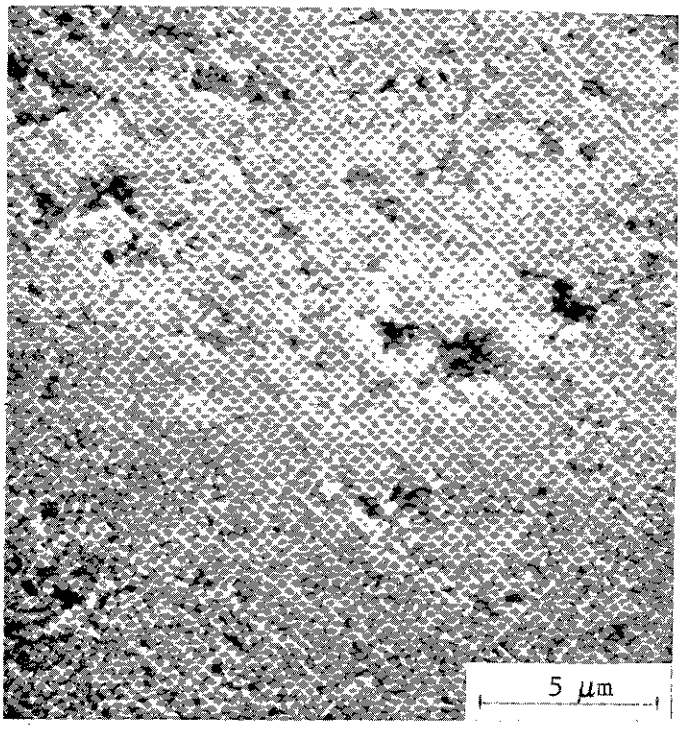

Figure 13. Incinerator ash from neoprene gloves magnified 100X, 500X, and 5000X

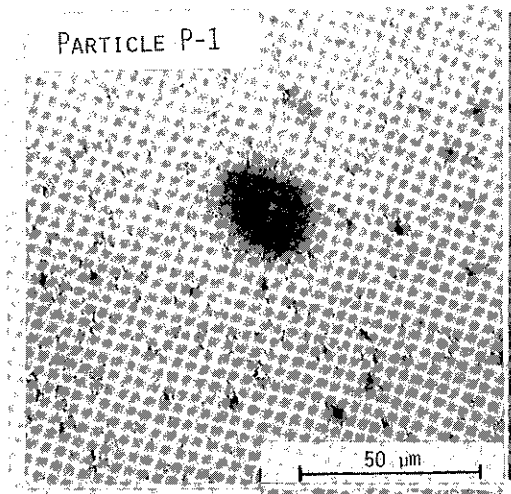

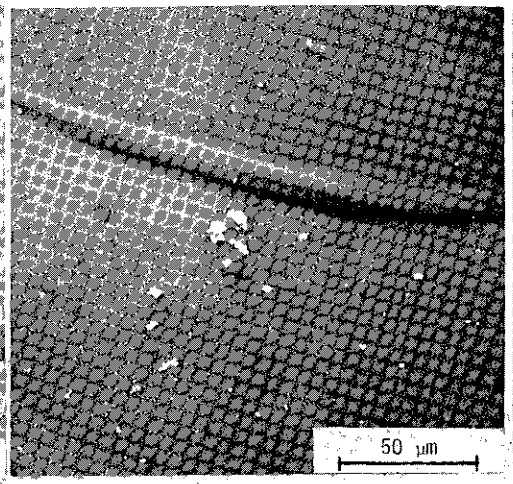

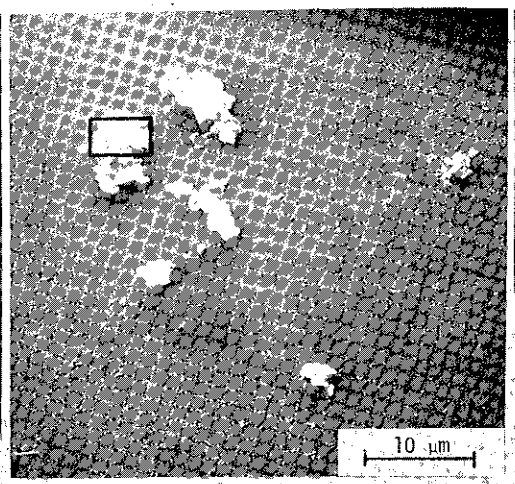

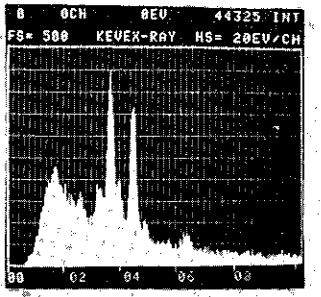

Al, Si, Ca, Ti, Fe

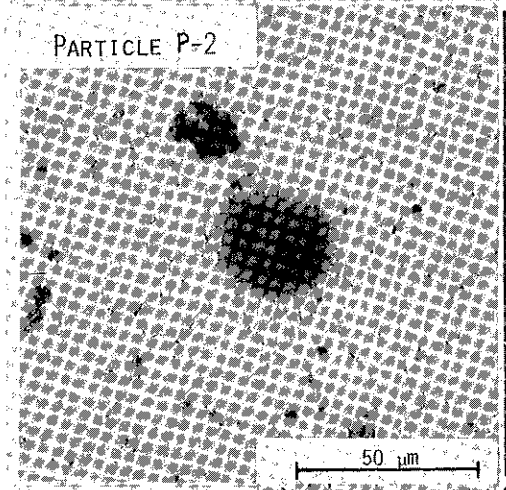

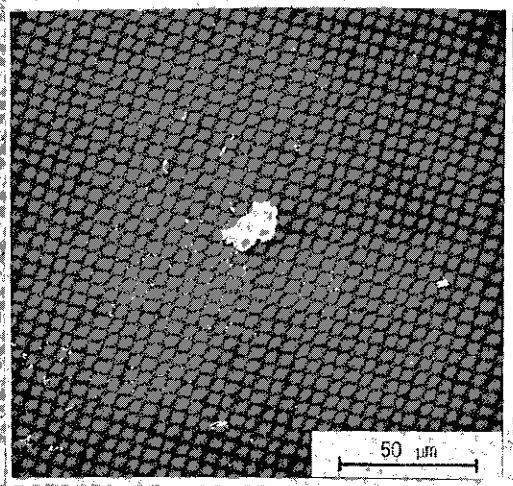

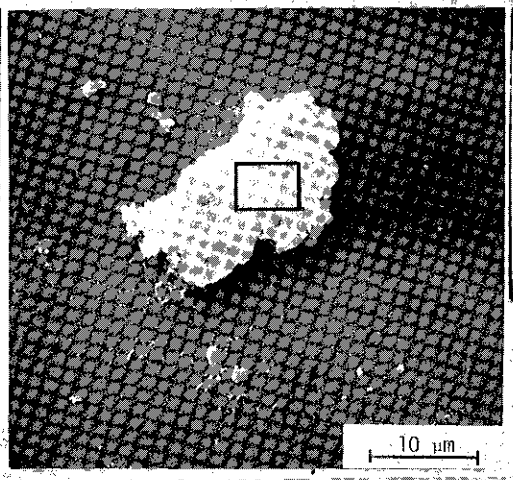

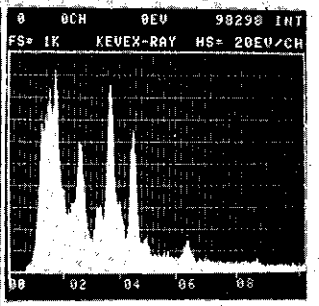

Mg, Al, Si, Cl, Ca, Ti, Fe

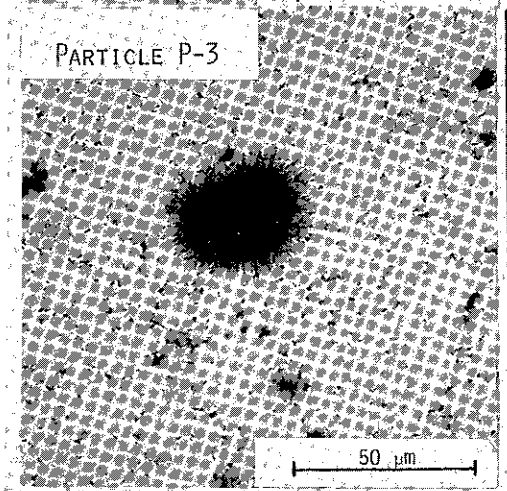

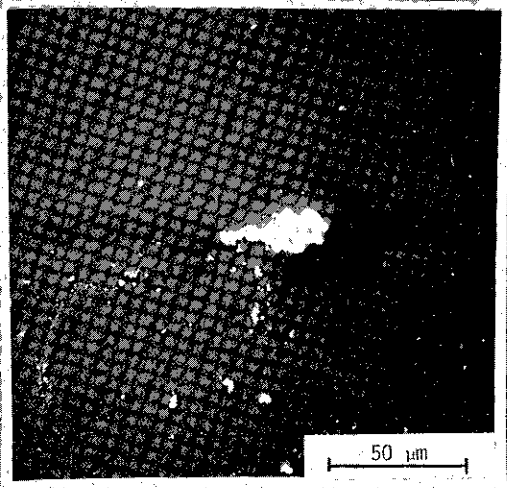

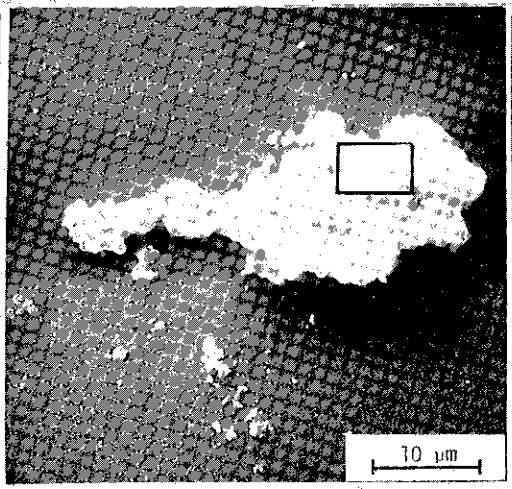

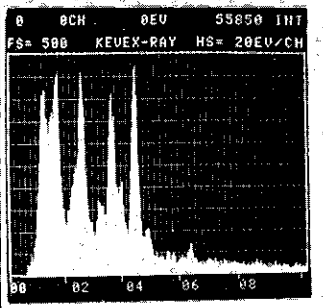

Mg, Si, Cl, Ca, Ti, Fe

Figure 14a.

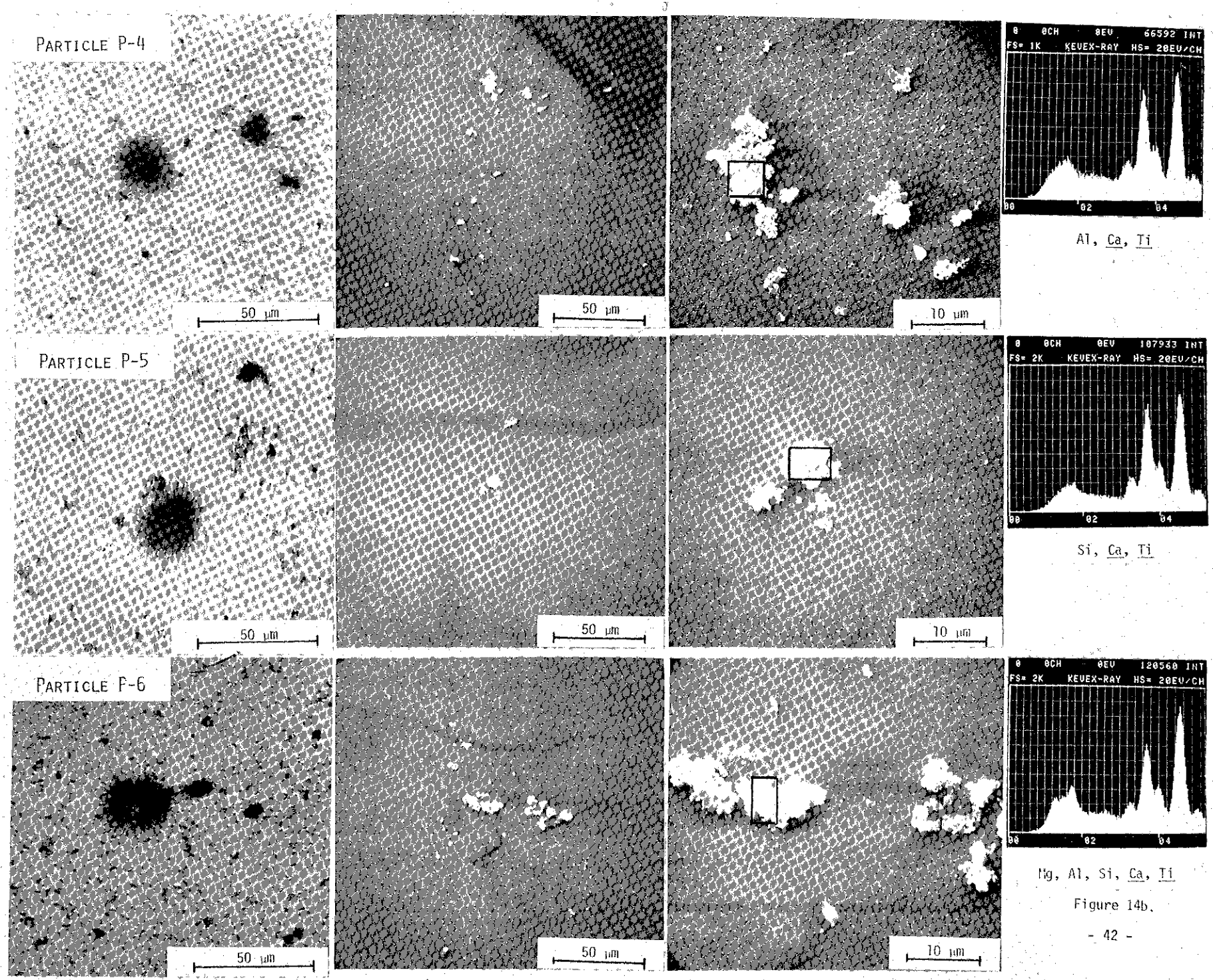
PARTICLE P-4
50 µm
50 µm
10 µm
0 0CH 0EV 66592 INT
FS= 1K KEVEX-RAY HS= 20EV/CH
00 02 04
Al, Ca, Ti
PARTICLE P-5
50 µm
50 µm
10 µm
0 0CH 0EV 107933 INT
FS= 2K KEVEX-RAY HS= 20EV/CH
00 02 04
Si, Ca, Ti
PARTICLE P-6
50 µm
50 µm
10 µm
0 0CH 0EV 120560 INT
FS= 2K KEVEX-RAY HS= 20EV/CH
00 02 04
Mg, Al, Si, Ca, Ti

Figure 14b.

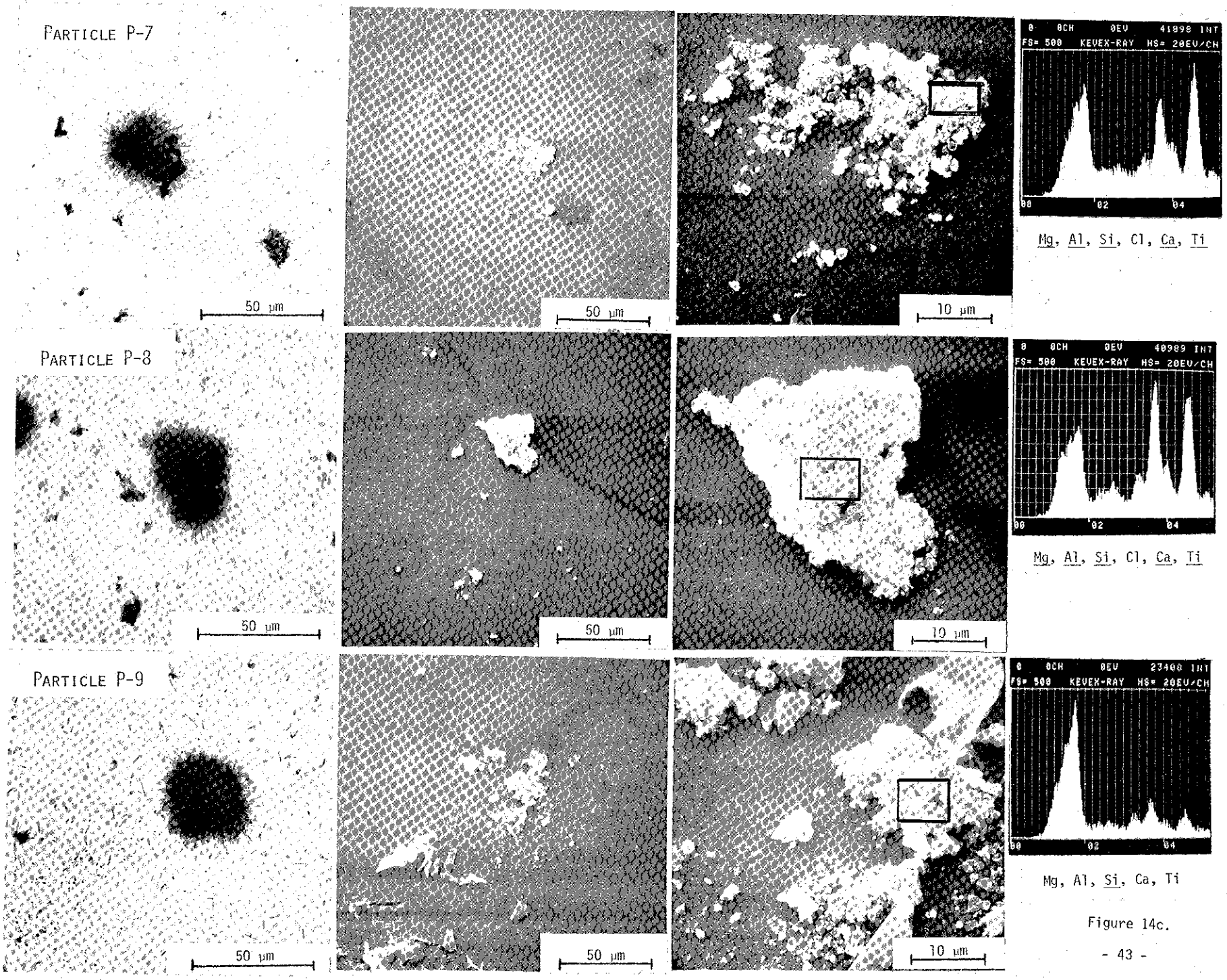
PARTICLE P-7
50 µm
50 µm
10 µm
0 0CH 0EV 41898 INT
FS= 500 KEVEX-RAY HS= 20EV/CH
00 02 04
Mg, Al, Si, Cl, Ca, Ti
PARTICLE P-8
50 µm
50 µm
10 µm
0 0CH 0EV 40989 INT
FS= 500 KEVEX-RAY HS= 20EV/CH
00 02 04
Mg, Al, Si, Cl, Ca, Ti
PARTICLE P-9
50 µm
50 µm
10 µm
0 0CH 0EV 23400 INT
FS= 500 KEVEX-RAY HS= 20EV/CH
00 02 04
Mg, Al, Si, Ca, Ti

Figure 14c.

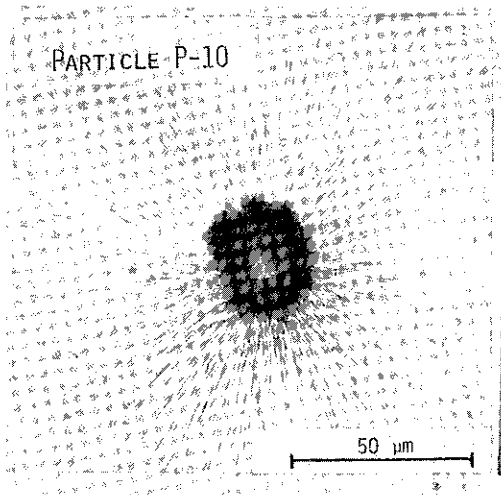

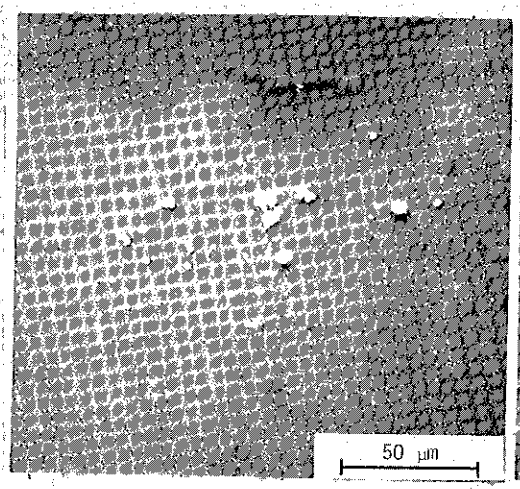

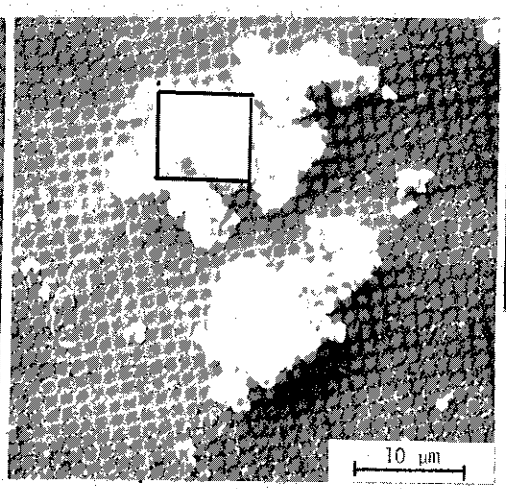

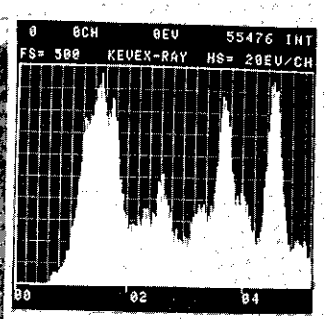

Mg, Al, Si, Cl, Ca, Ti

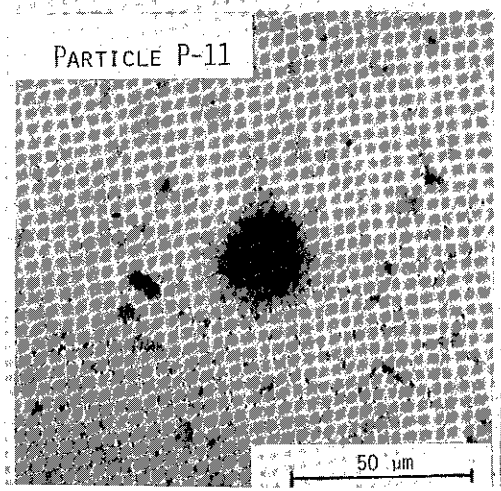

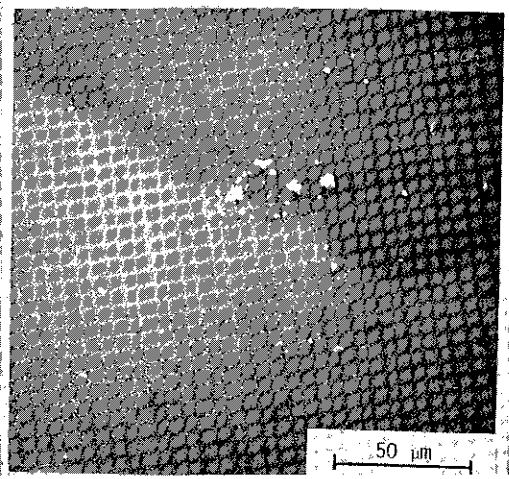

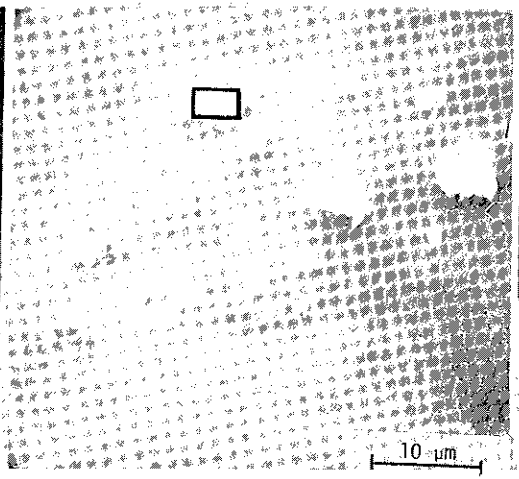

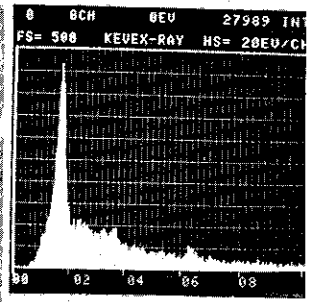

Si, Ca, Fe

Figure 14d.

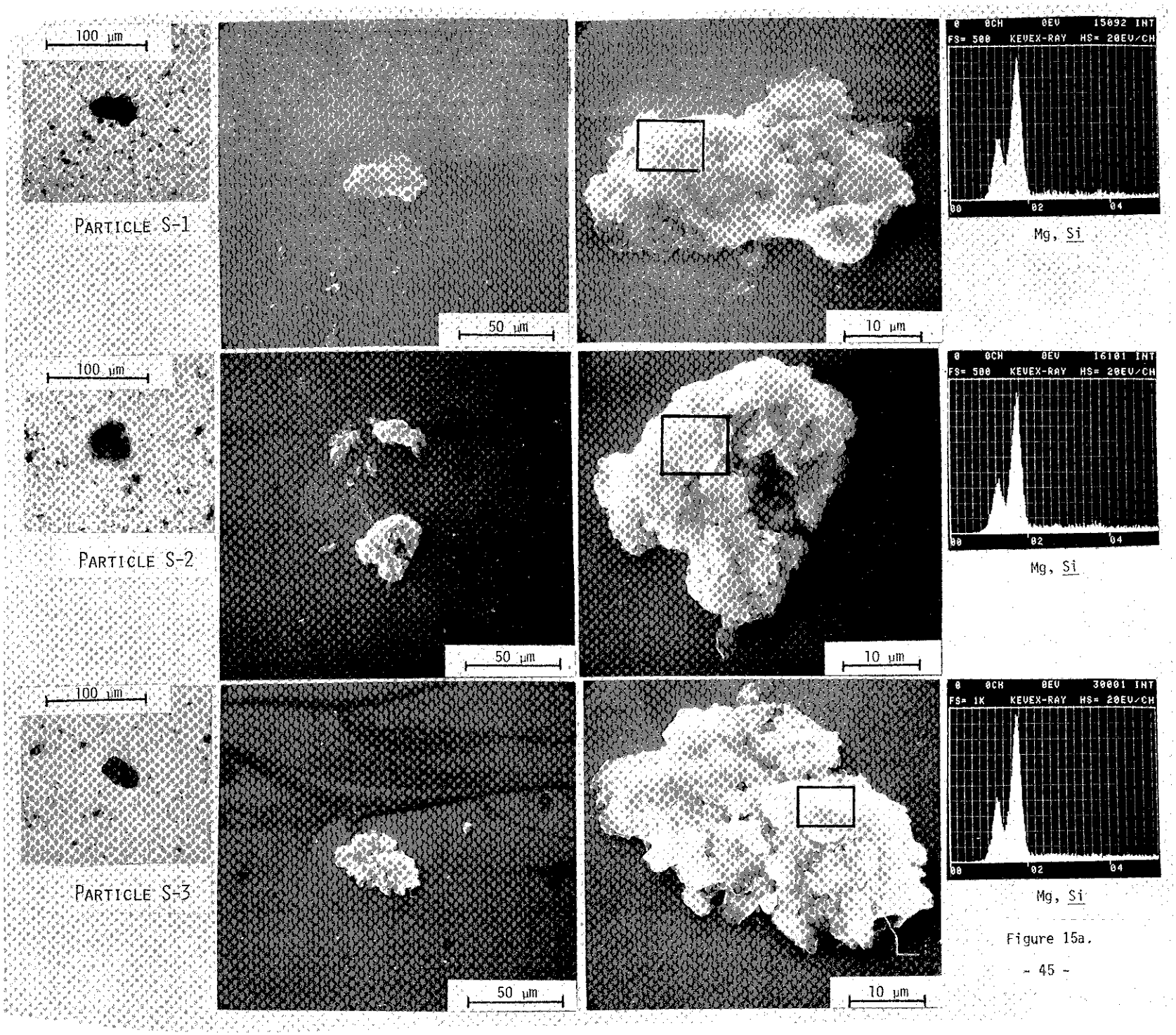
100 µm
PARTICLE S-1
50 µm
10 µm
0 0CH 0EV 15092 INT
FS= 500 KEVEX-RAY HS= 20EV/CH
00 02 04
Mg, Si
100 µm
PARTICLE S-2
50 µm
10 µm
0 0CH 0EV 16101 INT
FS= 500 KEVEX-RAY HS= 20EV/CH
00 02 04
Mg, Si
100 µm
PARTICLE S-3
50 µm
10 µm
0 0CH 0EV 30001 INT
FS= 1K KEVEX-RAY HS= 20EV/CH
00 02 04
Mg, Si

Figure 15a.

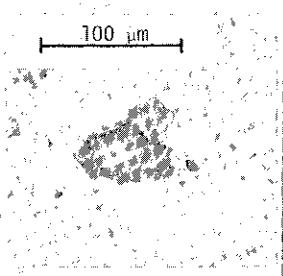

PARTICLE S-4

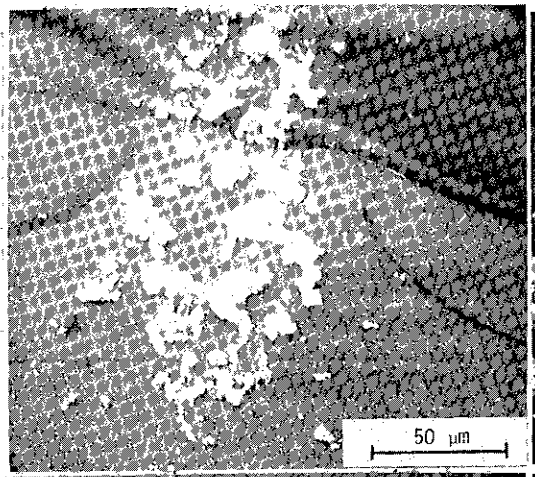

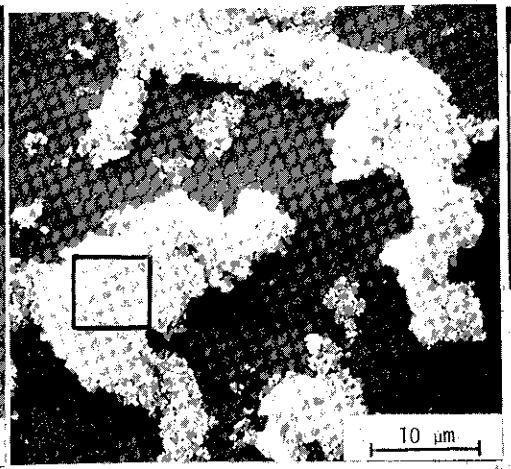

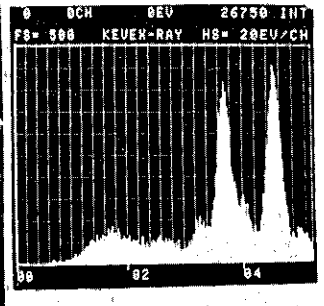

Ca, Ti

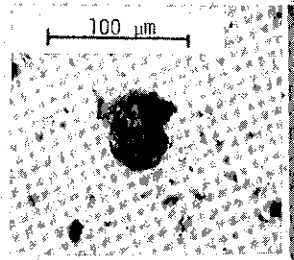

PARTICLE S-5

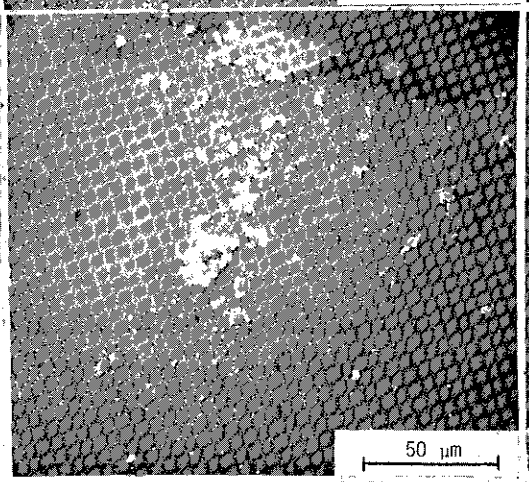

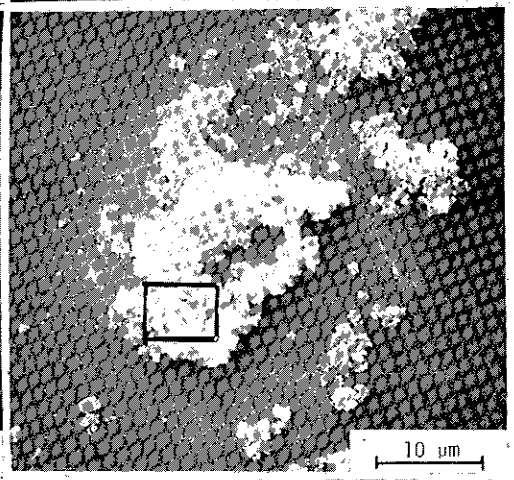

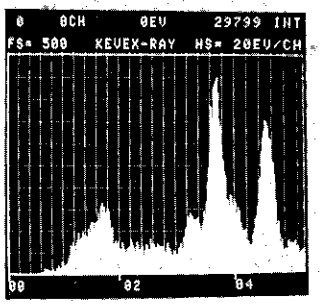

Si, Ca, Ti

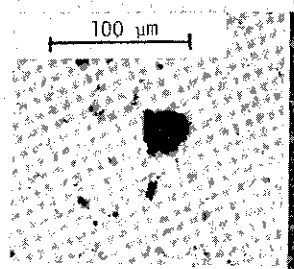

PARTICLE S-6

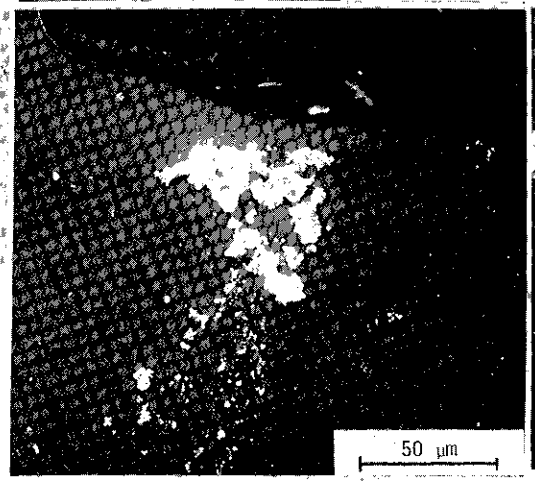

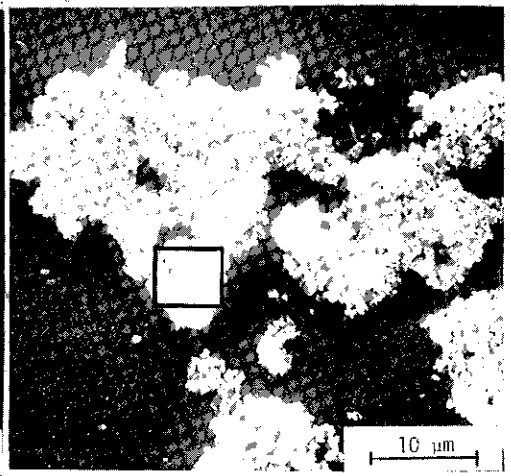

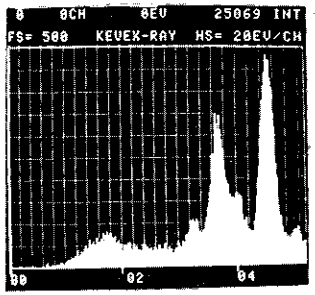

Ca, Ti

Figure 15b.

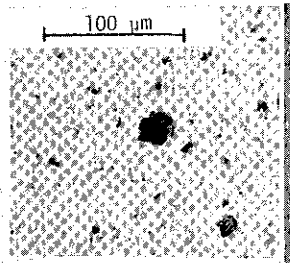

PARTICLE S-7

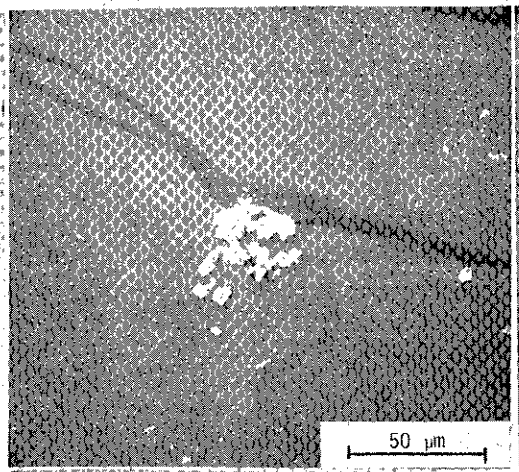

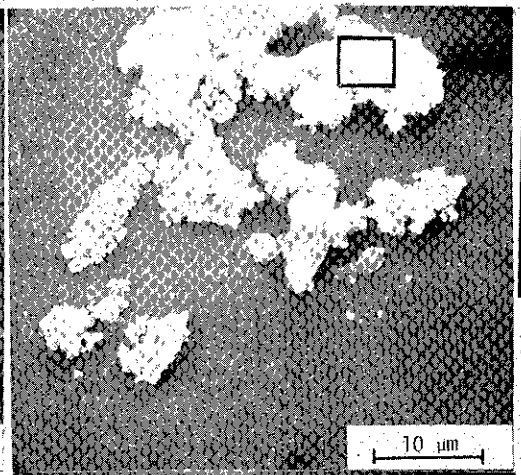

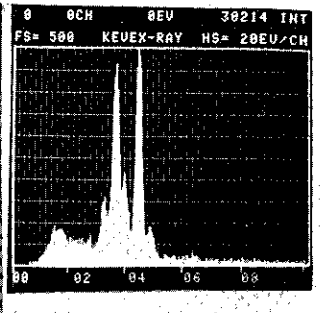

Si, Ca, Ti

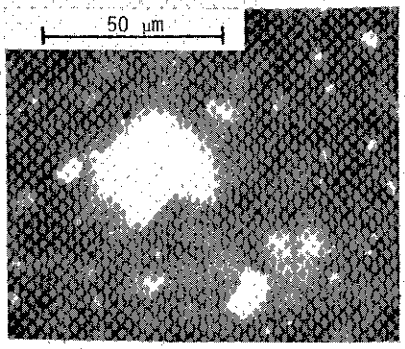

PARTICLE S-8

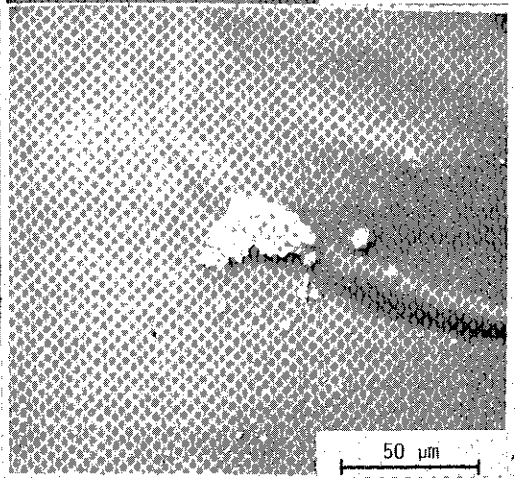

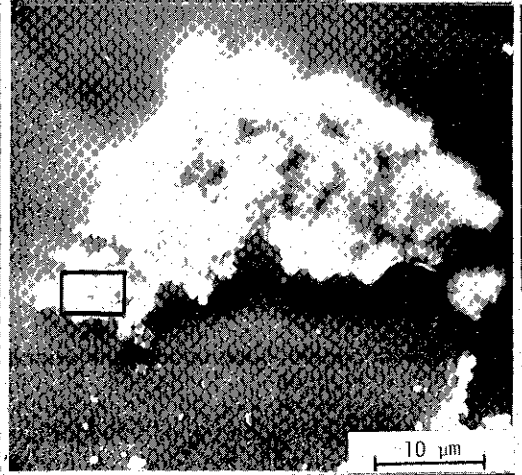

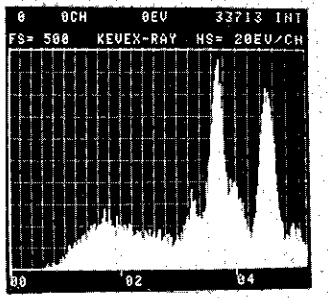

Ca, Ti

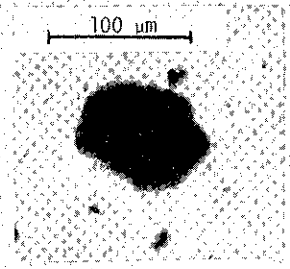

PARTICLE S-9

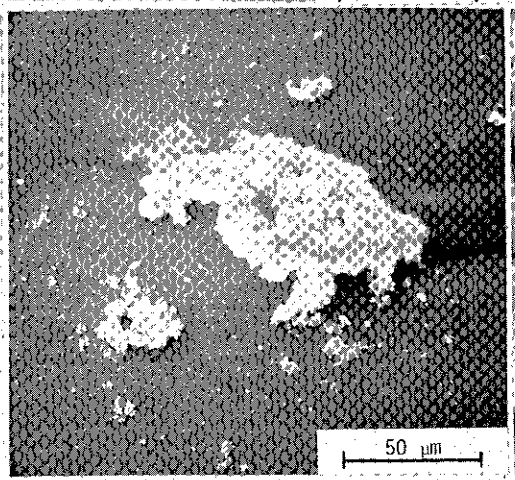

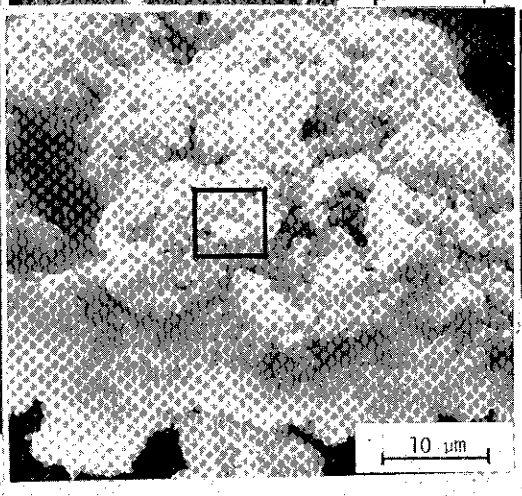

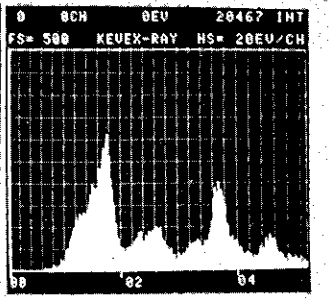

Mg, Al, Si, Cl, Ca, Ti

Figure 15c.

PARTICLE S-10

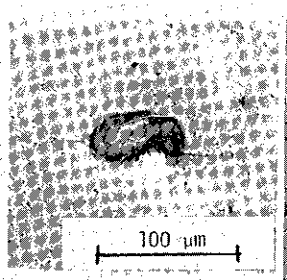

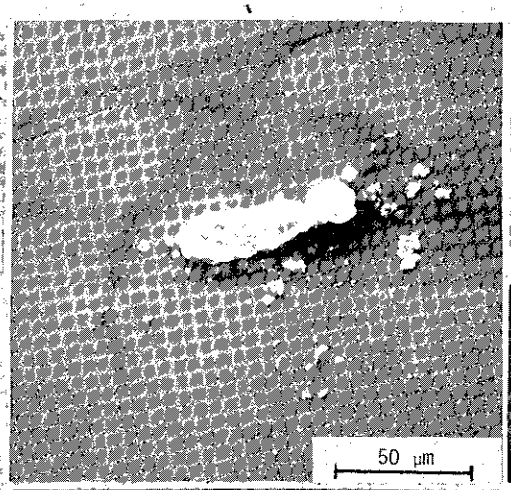

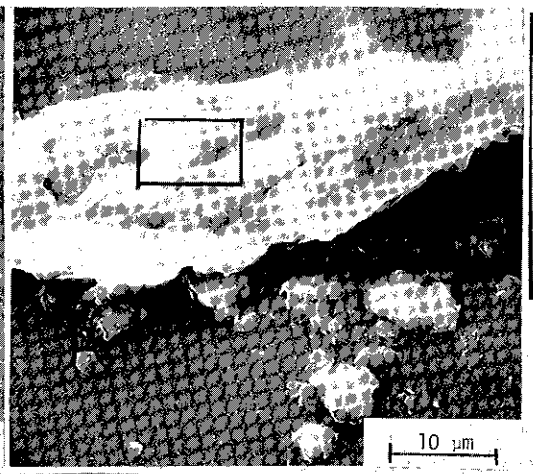

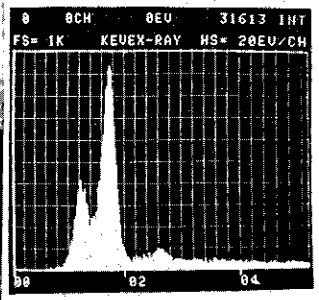

Mg, Si, Cl

PARTICLE S-11

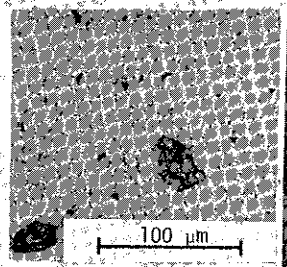

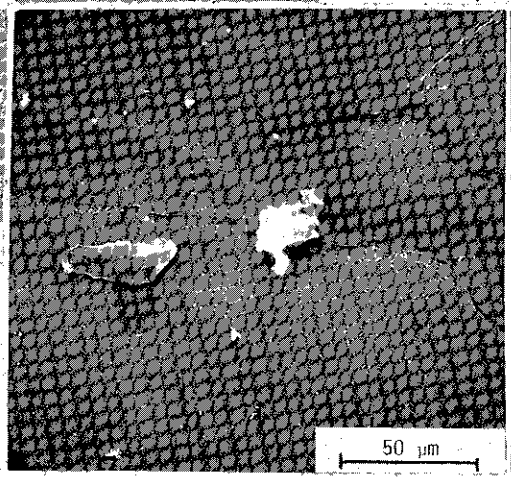

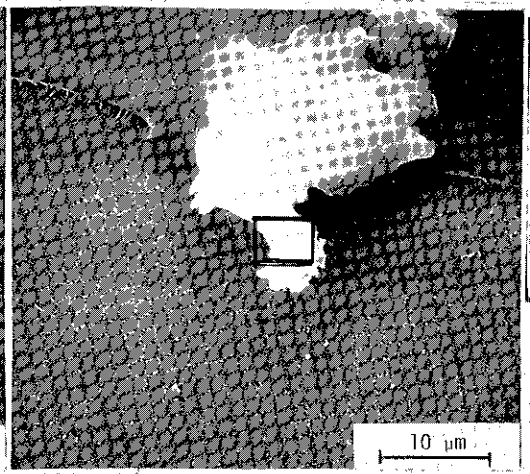

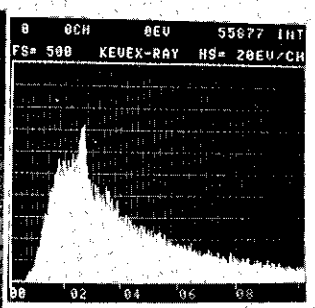

Cl

PARTICLE S-12

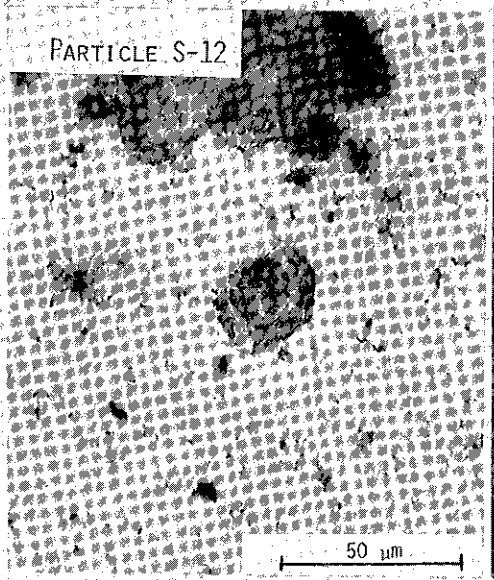

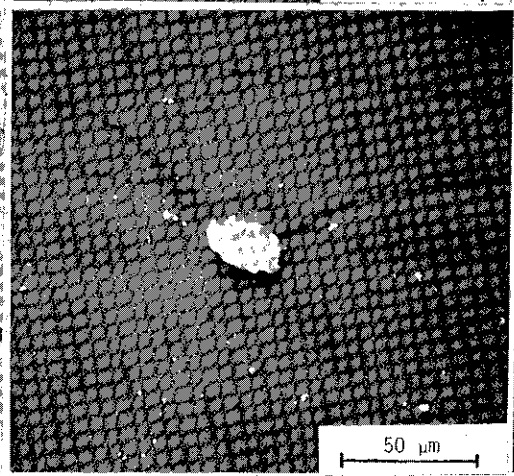

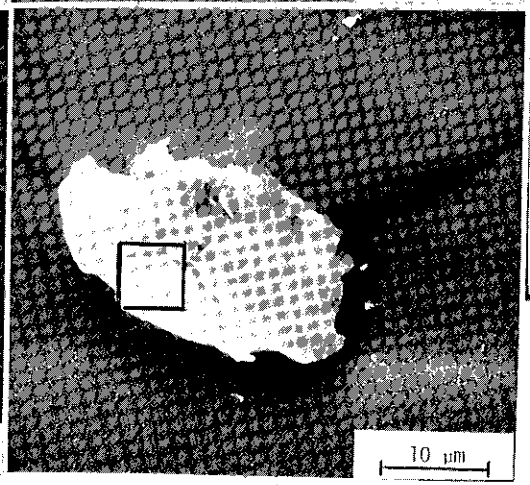

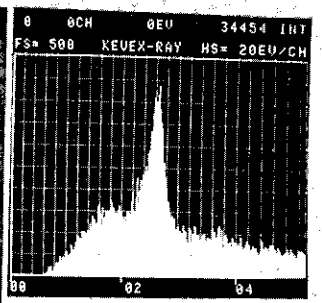

Ca, Cl

Figure 15d.

REFERENCES

1. G. M. Hidy and J. R. Brock. The Dynamics of Aerocolloidal Systems. New York: Pergammon Press, 1970.

2. Subcommittee on Airborne Particles of the Committee on Medical and Biologic Effects of Environmental Pollutants, National Research Council. Airborne Particles. Baltimore: University Park Prees, 1979.

3. R. Jaenicke, C. Junge, and H. J. Kanter. Messungen der Aerosolgrossenverteilung uber dem Atlantik. "Meteor" Forschungsergebnisse, Reihe B.7:1-54, 1971.

4. C. E. Junge. Air Chemistry and Radioactivity. New York: Academic Press, 1963.

5. H. P. Holcomb. Studies of Ashes Produced from Individual Solid Waste Components and a Standard Mixture Ignited at 1000°C, Letter to M. D. Boersma, May 1, 1978.

6. S. M. Sanders. Methodology for the Isolation and Characterization of Individual Plutonium-Bearing Particles in Atmospheric Effluents from a Nuclear Processing Plant. Nuclear Methods in Environmental and Energy Research, USERDA Report Conf-771072 pp 422-440, 1977.

7. S. M. Sanders. Characterization of Airborne Plutonium-Bearing Particles from a Nuclear Reprocessing Plant. Proceedings of the 15th DOE Nuclear Air Cleaning Conference. USDOE Report Conf-780819 Vol. 2 pp 708-736, 1978.

8. S. M. Sanders. Isolation and Characterization of Individual Plutonium-Bearing Particles in Atmospheric Effluents from a Nuclear Processing Plant, Health Physics:36, 371-385, 1979.

9. S. M. Sanders. The Detection and Study of Plutonium Particles Following the Reprocessing of Reactor Fuel. Transuranic Elements in the Environment. USDOE/OHER Report TID-22800, 1979.

10. W. C. McCrone and J. G. Delly. The Particle Atlas, Edition Two. Ann Arbor: Ann Arbor Science Publishers, Inc. 1973.

11. S. Katcoff, J. A. Miskel, and C. W. Stanley. Phys. Rev. 74: 631, 1948.